AD-A107 392 GENERAL ELECTRIC CORPORATE RESEARCH AND DEVELOPMENT --ETC F/G 20/3
INVESTIGATION FOR LOW-COST PERMANENT MAGNETS.(U)
SEP 81 J J BECKER
UNCLASSIFIED SMD-81-076 N00014-80-C-0566
NL

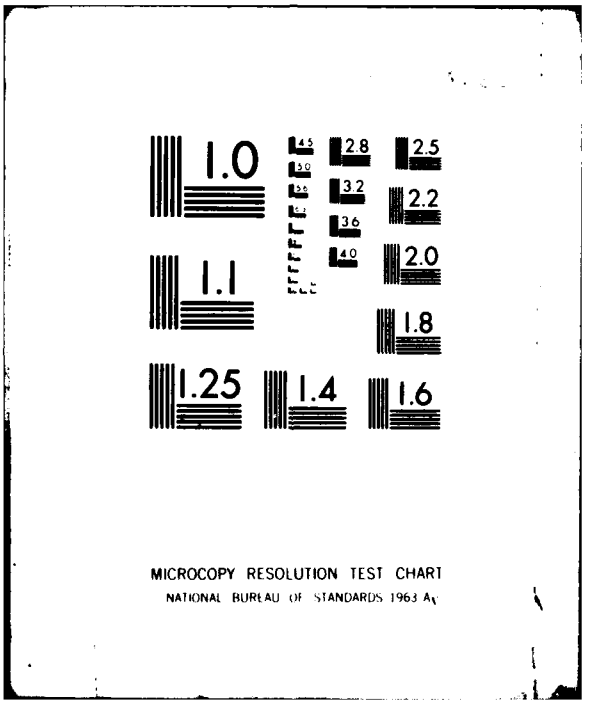
1.0
1.1
1.25
1.4
1.6
1.8
2.0
2.2
2.5
2.8
3.2
3.6
4.0
MICROCOPY RESOLUTION TEST CHART
NATIONAL BUREAU OF STANDARDS 1963 A

(12) LEVEL II

INVESTIGATION FOR LOW-COST PERMANENT MAGNETS

Annual Report

Contract N00014-80-C-0566

Prepared for

Department of the Navy
Office of Naval Research
Arlington, Virginia 22217

Prepared by

Properties Branch
Metallurgy Laboratory
Corporate Research and Development
General Electric Company
Schenectady, NY 12301

September 1981

Approved for public release; distribution unlimited

SECURITY CLASSIFICATION OF THIS PAGE (When Data Entered)

REPORT DOCUMENTATION PAGE		READ INSTRUCTIONS BEFORE COMPLETING FORM
1. REPORT NUMBER	2. GOVT ACCESSION NO. AD-A107 392	3. RECIPIENT'S CATALOG NUMBER
4. TITLE (and Subtitle) INVESTIGATION FOR LOW-COST PERMANENT MAGNETS.		5. TYPE OF REPORT & PERIOD COVERED Annual Report 1 July 1980 — 30 June 1981
		6. PERFORMING ORG. REPORT NUMBER SRD-81-076
7. AUTHOR(s) J.J. Becker		8. CONTRACT OR GRANT NUMBER(s) N00014-80-C-0566
9. PERFORMING ORGANIZATION NAME AND ADDRESS General Electric Company Corporate Research and Development Schenectady, New York 12301		10. PROGRAM ELEMENT, PROJECT, TASK AREA & WORK UNIT NUMBERS
11. CONTROLLING OFFICE NAME AND ADDRESS Department of the Navy Office of Naval Research Arlington, Virginia 22217		12. REPORT DATE September 1981
		13. NUMBER OF PAGES 40
14. MONITORING AGENCY NAME & ADDRESS (if different from Controlling Office)		15. SECURITY CLASS. (of this report) Unclassified
		15a. DECLASSIFICATION/DOWNGRADING SCHEDULE

16. DISTRIBUTION STATEMENT (of this Report)

Approved for public release; distribution unlimited.

17. DISTRIBUTION STATEMENT (of the abstract entered in Block 20, if different from Report)

18. SUPPLEMENTARY NOTES

19. KEY WORDS (Continue on reverse side if necessary and identify by block number)

amorphous materials, magnetic materials, permanent magnets, crystallization

20. ABSTRACT (Continue on reverse side if necessary and identify by block number)

The crystallization of initially amorphous rapidly quenched alloys may provide new materials with good permanent magnet properties at low cost. Preliminary investigations indicate that phosphorus and carbon are favorable alloying elements, and that sudden changes in properties may occur as the identities of the crystallizing phases change. The exploration of alloy systems has been greatly speeded up by the use of current-pulse annealing. It has been found that remanence ratios may be quite high even though the orientation of the crystals formed is probably random. The course of crystallization has been followed by resistance monitoring in conjunction with current-pulse annealing. X-ray diffraction indicates that the highest coercive forces are attained in only partially

DD FORM 1 JAN 73 1473 EDITION OF 1 NOV 65 IS OBSOLETE

UNCLASSIFIED

SECURITY CLASSIFICATION OF THIS PAGE (When Data Entered)

20. Abstract

crystallized samples. Magnetic domain structures have been studied in crystallized ribbons and also in bulk samples of some of the phases observed in them, using both Kerr effect and magnetic colloid. These studies have given useful information about the nature and the magnitude of the magnetocrystalline anisotropy in the phases formed. Alloys containing rare earth elements appear very promising and are being actively pursued.

TABLE OF CONTENTS

Introduction

This report covers the work done on Contract N00014-80-C-0566 during the period 1 July 1980 through 30 June 1981. The objective of this work was to investigate crystallized amorphous metals as a new class of permanent magnet materials with potentially high or moderate properties at low cost. This was done by the means set forth in the work statement. In brief, they are:

1. Preparation of samples by rapid solidification of molten metal, followed by heat treatments to develop optimum permanent magnet properties. Exploration of the variation of magnetic properties with composition.

2. Determination of the phases and structures formed on annealing by microscopy, diffraction, and magnetic domain structure observations. Study of the kinetics and mechanisms of crystallization by thermal and thermomagnetic analysis.

3. Analysis of magnetization curves and hysteresis loops to yield information about the compositions and structures of the phases formed. Studies of such phases prepared in bulk.

4. Theoretical studies of the influence of microstructure and anisotropy on coercive force and remanence.

This report gives some background to this work, reviews our accomplishments during the stated period, and indicates the direction the work is now taking.

The work in the current period has resulted in four presentations and two papers published in technical journals. These papers and digests are incorporated into this report.

High-Anisotropy Materials

A useful permanent magnet material must combine a reasonably high saturation magnetization $4\pi M_s$ with a large coercive force H_c. The latter is generally associated with a high magnetocrystalline anisotropy. Before the advent of amorphous metals, a search had been carried out at the General Electric Research and Development Center for intermetallic compounds that might combine high magnetization with high anisotropy. A number of interesting compounds, including borides, phosphides, stannides, carbides, and germanides, were prepared by conventional metallurgical techniques, which was often difficult. A summary of the properties found is given in Table I.

Compound	T_c / °C	Room T Sat. / Gauss	Room T H_c Observed / Oersteds
Fe_3Sn	470	12,300	201
Fe_3Ge	382	14,900	—
Fe_5Ge_3	212	7,180	432
Fe_3P	508	13,900	220
Fe_3C	217	13,700	230
Fe B	335	8,300	24
$Fe_{0.5}Mn_{0.5}B$	513	10,270	295
Mn B	330	13,100	53
Fe_3B	518	14,800	—

Table I - Summary of intermetallic compounds combining high-magnetization high-anisotropy properties.

These results suggest some potentially interesting materials, although many of them are difficult to prepare. At this point the enormous magnetocrystalline anisotropy of Co_5Y became known, and the large coercive forces shown by Co_5Sm were discovered in this laboratory. Research and development were then concentrated on the cobalt-rare-earths, culminating in a new class of commercial materials with properties far beyond anything previously attainable, but, of course, relying on costly and strategic materials.

Crystallized Amorphous Materials

In our studies of amorphous materials, which began in 1974, one of our concerns has been the effect of annealing treatments on the soft magnetic properties. When a temperature is reached at which crystallization begins, typically 400-500°C, the coercive force H_c rises rapidly and the outstanding soft magnetic properties are lost. However, it appeared to us that at times H_c could rise to values high enough to be interesting and useful as a permanent magnet material. For example, an amorphous $Fe_{40}Ni_{40}P_{20}$ alloy, as prepared, had an H_c of 0.05 Oe (Oersteds). When it was crystallized, its H_c was 365 Oe. This material has $4\pi M_s$ of 8850 G (Gauss). An amorphous Fe-B alloy, with $4\pi M_s$ of 14,300 G, was annealed to an H_c of 110 Oe. Preliminary numbers of this sort strongly indicated a high potential for useful permanent magnet materials, especially considering that these alloys contain no cobalt. For comparison, Alnico IIIC, which also contains no cobalt, has a remanence B_r of 7500 G and an H_c of 400 Oe. Its maximum energy product $(BH)_m$ is only 1.35 MGOe (million gauss-oersteds), which is low because this material is isotropic. The Alnicos that contain 24% cobalt have H_c varying from 580 to 1100 Oe, B_r of 7500 to 13,400 G, and $(BH)_m$ of 2.75 to 7.5 MGOe. Barium ferrites have B_r up to 2000 G and $(BH)_m$ of <1 MGOe in plastic-bonded form, and up to 4000 G and 3 MGOe in sintered form. In spite of these modest properties they find considerable application because of their low cost. An intermetallic compound with $4\pi M_s$ of 10,000 G and H_c of 500 Oe, packed to 80% density and 80% aligned, would have $(BH)_m$ in the vicinity of 3 MGOe. Such material would be extremely useful, particularly as it might well contain no cobalt and be made from inexpensive material.

Guided by these considerations, we made a preliminary investigation of a large number of alloys. Melt-quenched ribbons were annealed for 15 minutes at 525°C, which may not have been optimum for every alloy but probably did not completely miss any significant candidates. The results of this survey are summarized in Table II, for alloys containing no cobalt, and Table III, for alloys with cobalt.

In a number of cases additional temperature runs were made. The general conclusions that could be drawn from this survey were the following:

1. For non-cobalt-containing alloys, phosphorus and carbon seemed to lead to higher H_c than boron.
2. In a number of cases there were abrupt changes in H_c with composition.
3. In many Co-bearing alloys the crystallized materials gave hysteresis loops showing clearly the presence of two phases of different magnetic properties.

Fe	Ni	P	B	C	Si	Cr	V	H_c
70	10	20						50
65	20	15						80
60	20	20						43
50	30	20						35
42.5	42.5	15						200
43	43	16						220
41.5	41.5	17						175
40	40	20						365
30	50	20						285
20	60	20						275
43	43		14					25
41	41		18					23
40	40		20					40
38	38		24					24
30	50		20					33
41	42.4	16	0.6					330
40	40	17	3					116
40	40	14		6				53
80		14	6					68
70	10	14	6					23
70	10	14		6				124
60	20	14	6					68
40	40	14	6					53
40	40	14		6				330
80		5	15					43
80			15	5				29
72			28					84
74			26					87
76			24					23
78			22					24
80			20					21
82			18					13
84			16					11
85			15					9
86			14					45
88			12					54
92			8					45
75			10		15			33
84		15			1			69
81		15			4			89
85			14		1			67
84			8	4	4			51
81.5			14.5		4			58
76			18				6	13
75		14	6			5		24
80		10	10					20
65	20	10	5					61
82		15			3			46
81		12		7				18
80			10	10				26

Table II - Survey of melt-quenched alloys without cobalt and resulting H_c after annealing at 525°C for 15 minutes.

Fe	Ni	Co	P	B	H_c
		72		28	82
		74		26	107
		76		24	44
		77		23	24
		78		22	32
		80		20	104
		82		18	470
		83		17	290
		84		16	390
38		38		24	27
40.5		40.5		19	38
41		41		18	23
42		42		16	14
42.5		42.5		15	14
43		43		14	13
53		30		17	78
60		20		20	31
50		30		20	21
20		60		20	85
45		45	10		102
41		41	18		222
40		40	20		315
39		39	22		312
38		38	24		360
	40	40		20	92
28	28	28		16	64

Table III - Survey of melt quenched alloys with cobalt and resulting H_c after annealing at 525°C for 15 minutes.

All of these observations clearly pointed to the need of better understanding of three things:

1. The mechanism and kinetics of the crystallization process, which determine the identity and morphology of the phases produced;

2. The magnetic properties of the phases being formed;

3. The relationship of magnetic properties to the structure of partially or totally crystallized materials.

The highest H_c obtained in this preliminary survey for a non-cobalt-containing alloy was 365 Oe for $Fe_{40}Ni_{40}P_{20}$. At that time the highest value for any alloy was 470 Oe for $Co_{82}B_{18}$. Since then, these values have been increased to 420 and 830 Oe, as described below. These are very respectable coercive forces, covering most of the range of the Alnicos. Such coercive forces could well be the basis for a widely useful family of materials.

A number of cobalt-containing alloys exhibited very clear-cut two-phase hysteresis loops and clearly defined domain structures. Thus it appeared useful to continue investigating some of them as an effective means toward the understanding of the coercivity mechanism. In our continuing work, the techniques of light and electron microscopy, diffraction, calorimetry, and hysteresis loop analysis have been supplemented by resistivity measurements of the transforming alloy, and by magnetic domain observations, both in crystallized amorphous materials and in crystalline phases prepared in bulk.

Current-Pulse Annealing

The exploration of alloy systems has been greatly speeded by the use of current-pulse annealing. In this technique ribbons are annealed by short ($\approx$1 sec) pulses of successively greater current. In this way it is possible to locate high H_c maxima for crystallized amorphous metals, as in Figure 1, the entire experiment taking only a few minutes. The highest H_c found in this way was consistently higher than that found isothermally in a given alloy. This may be associated with the rapid rate of temperature rise. Some comparative values are shown in Table IV. The value of 420 Oe for $Fe_{40}Ni_{40}P_{20}$ shown in the table is the highest so far for a non-cobalt-containing alloy. The highest H_c seen was 830 Oe in another run on the material shown in Figure 1.

High Remanence Ratios

A very important phenomenon has been observed in annealed ribbons of a number of alloys. The ratio of remanence to saturation of the ribbon as annealed is much

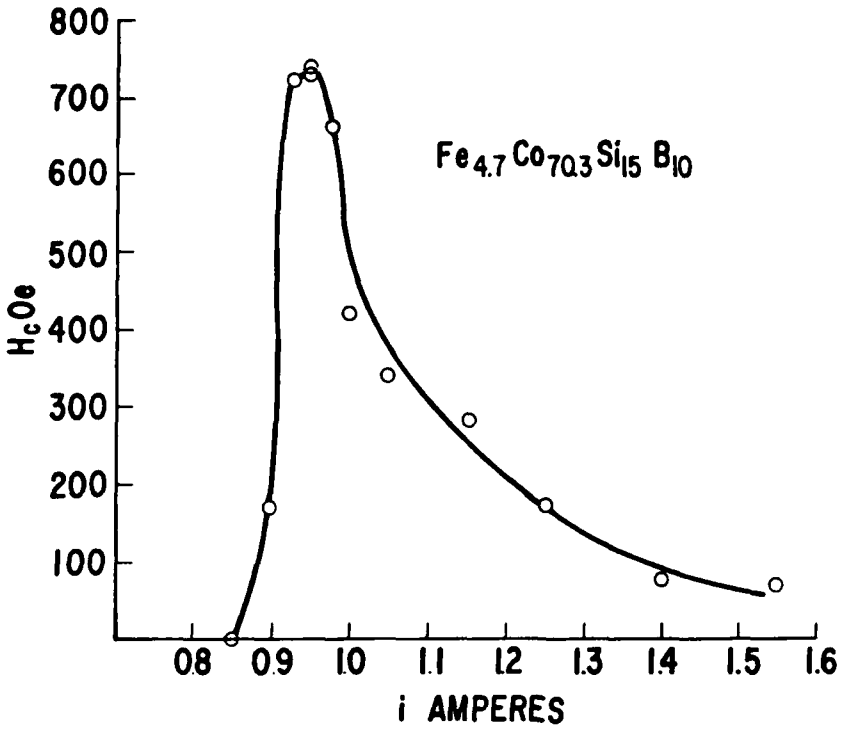

Figure 1 - Coercive force resulting from successive 1-second annealing pulses of increasing current in an initially amorphous $Fe_{4.7}Co_{70.3}Si_{15}B_{10}$ alloy.

Composition	Current-Pulse H_c	H_c at 525°C for 15 Minutes	Best Isothermal H_c
$Fe_{40}Ni_{40}P_{20}$	420	365	365
$Fe_{70}Ni_{10}P_{14}C_6$	181	124	—
$Fe_{63}Co_{20}B_{17}$	200	78	159
$Co_{82}B_{18}$	580	470	470
$Co_{77}B_{23}$	400	24	—

Table IV - Comparative H_c values for selected compositions using pulse-annealing, and at 525°C for 15 minutes.

higher than 0.5 and, for example, in the alloy shown in Figure 1, may be more than 0.8. If the structure consisted of a random distribution of particles with uniaxial anisotropy, the remanence would be at most 0.5, each particle saturated in the easy direction nearest to the magnetizing field. Higher values imply either that there is a strong crystallographic alignment, which seems unlikely, or that the crystal symmetry is higher, with multiple nearly equivalent easy directions, as might well be the case in some of these materials. Calculations indicate that the remanence can vary from 0.5 to 0.87 depending on the distribution of easy directions. This has the important practical consequence that a material with both high symmetry and high anisotropy would not need to be aligned for good properties, and they would be equally good in all directions. All of the best permanent magnet materials now in use are aligned by one means or another. This step is both crucial and difficult, and improves the properties in the alignment direction at the expense of those transverse to it.

Resistance Monitoring

The resistance of a ribbon being pulse annealed shows very significant changes. Figure 2 shows this behavior for the same alloy shown in Figure 1. The initial hold and subsequent drop in R/R_o indicate different crystallization processes. If now H_c is plotted as a function of R/R_o, as in Figure 3, it can be seen that the maximum in H_c occurs at an intermediate value. The results of x-ray diffraction are also indicated on Figure 3, with the important result that the high H_c occurs when the material is only partially transformed from the amorphous to the crystalline state. The crystalline phase present in this condition in this particular alloy has not yet been identified, but the fact that the remanence ratio is 0.82 strongly suggests that it is not single-easy-axis.

In an alloy of $Fe_{50}Co_{30}B_{20}$, the transformation curve, as shown in Figure 4, is characterized by a practically discontinuous and very reproducible initial drop. Crystallization is complete, into an $(Fe, Co)_3B$ structure, with a low H_c. It has not been possible to produce a partially crystallized sample. Further pulse annealing changes the structure to $(Fe, Co)_2B + \alpha$, with H_c an order of magnitude higher. $(Fe_{62.5}Co_{37.5})_2B$ is known to have single-easy-axis anisotropy.[1]

Rare Earths

Alloys of various Fe-B-Tb-La compositions have been prepared and ribbons are beginning to be made from them, following some work recently reported by Koon, Williams, and Das.[2] It appears that rare earths may provide performance-to-cost benefits in crystallized amorphous materials and this possibility is incorporated into our future work.

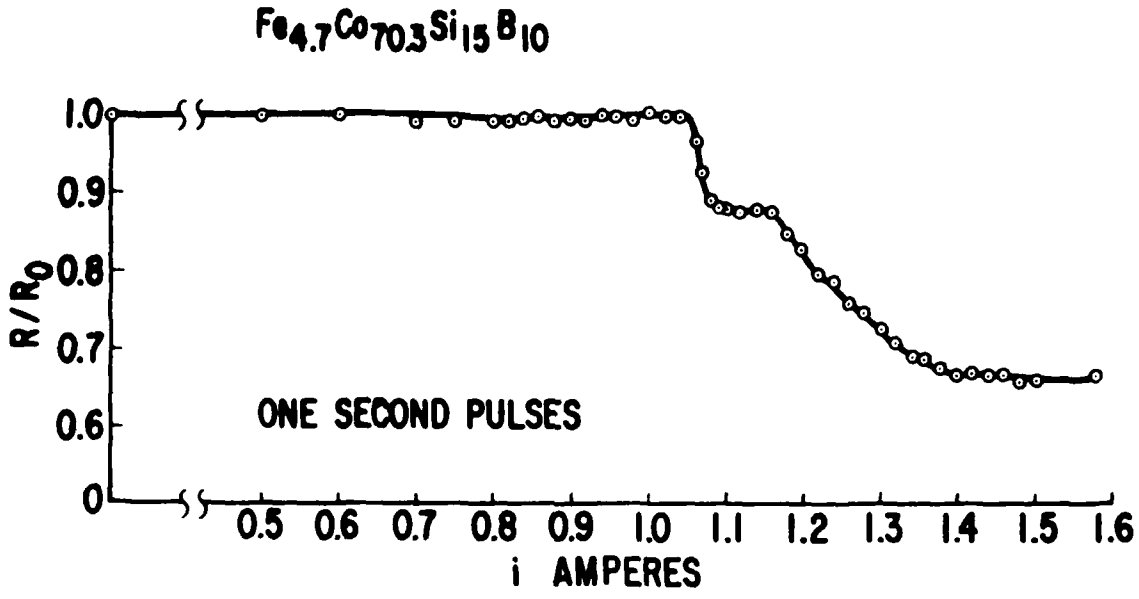

Figure 2 - Resistance monitoring of $Fe_{4.7}Co_{70.3}Si_{15}B_{10}$ during pulse annealing.

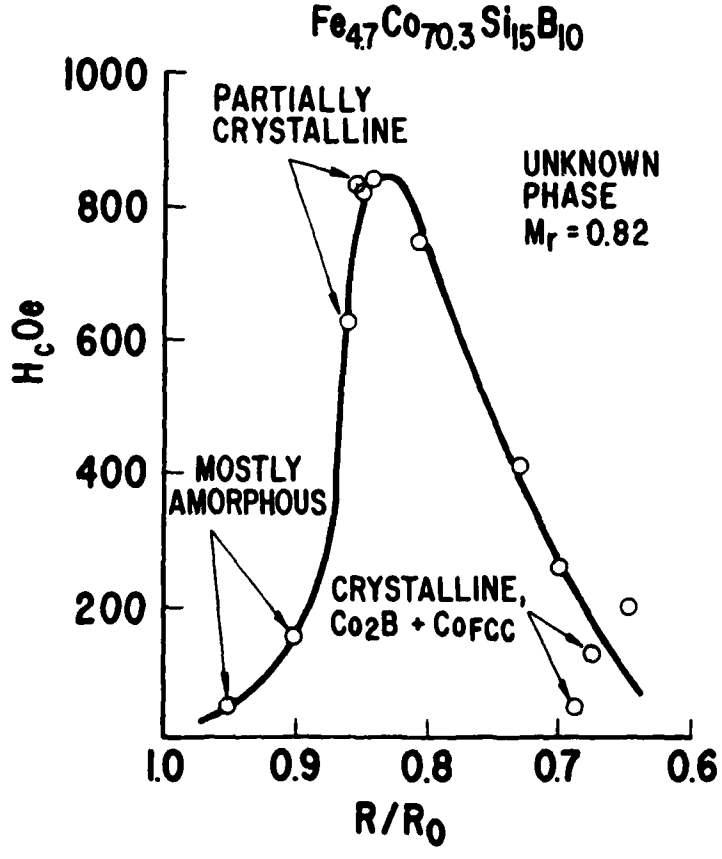

Figure 3 - Relationship of H_c to R/R_o of $Fe_{4.7}Co_{70.3}Si_{15}B_{10}$.

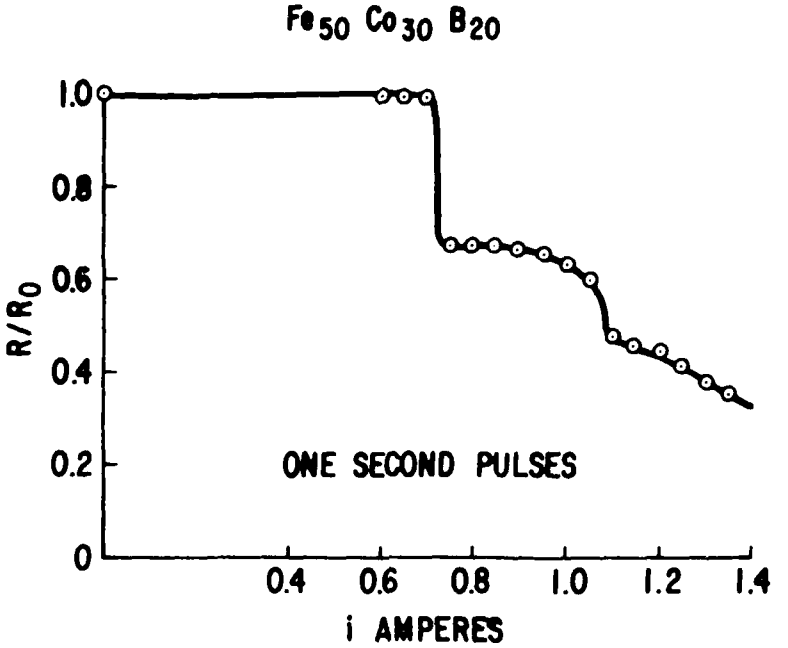

Figure 4 - Resistance monitoring of $Fe_{50}Co_{30}B_{20}$ during pulse annealing.

RFe_2 compounds in crystalline form have been found to have enormous room-temperature magnetostriction,[3] suggesting that their anisotropy may be high, and indeed $DyFe_2$ and $TbFe_2$ have anisotropy constants of the same order as those of Co_5Sm[4]. However, the RFe_2 phases are cubic. Again, this raises the possibility that permanent magnets based on such materials might not require alignment since the remanence ratio of the randomly oriented phase should exceed 0.8.

Amorphous RFe_2 compounds have been prepared by sputtering. Amorphous $TbFe_2$ is the first amorphous material whose magnetic structure has been studied by neutron diffraction.[5] At liquid helium temperatures these alloys show very large coercive forces, since the local anisotropy dominates the exchange interaction.[6] At room temperature its coercive force is small. However, Clark[7] annealed amorphous $TbFe_2$ at various temperatures and observed that the room-temperature H_c suddenly increased to 3400 Oe for an annealing temperature of 350°C, producing a material with a $(BH)_m$ of 7 MGOe. In this state it appears to be partially crystalline.

Croat, Chraplyvy, and Herbst[8] have reported on the crystallization of amorphous $Pr_{27}Co_{73}$, also prepared by sputtering. They found, as a function of annealing temperature, a rapid increase in H_c to a sharp peak followed by a steep decline. The

highest value they attained was 6800 Oe. Again, this value seems to correspond to partial crystallization.

Koon et al.[2] attempted to add Dy to a Fe-B amorphous alloy to investigate magnetostriction. They found that this induced cast-in crystals, but that La could be added without rendering the ribbon crystalline, and furthermore that the presence of La made it possible to add other rare earths as well. They prepared an amorphous quenched ribbon of $(Fe_{.82}B_{.18})_{.9}Tb_{.05}La_{.05}$ and then annealed it, attaining H_c of 7.3 kOe. Again, in this state it was only partially crystallized.

Domain Studies

Study of magnetic domain structures in ferromagnetic materials can be useful in identification of phases and in determination of the size and orientation of grains. It can also reveal the magnetic symmetry (e.g., easy-axis vs. easy-plane) of specific phases and can yield data on domain-wall energy and magnetocrystalline anisotropy.

Crystallization of amorphous Co-B or Fe-B ribbons generally leads to the formation of orthorhombic Co_3B and tetragonal Fe_3B phases, whose magnetic symmetries were unknown prior to this study. We have studied magnetic domain structures in these and related ternary phases, using both the polar Kerr technique (polarized light in normal incidence) and the Bitter technique (domain-wall decoration by magnetic colloid). In order to study the thermodynamic stability of the various phases, we have studied alloys as chill-cast, after annealing, and in the directionally-solidified condition, in addition to samples of crystallized amorphous ribbon.

The orthorhombic Co_3B phase exhibited a strong polar Kerr effect and showed domain structures similar to those of Co and Co_5Sm, characteristic of easy-axis magnetic symmetry. The domain structure in crystallized Co-24 at pct B ribbon is shown in Figure 5. From the average domain width in such pictures, a domain-wall energy 17 ergs/cm^2 was estimated. This is intermediate between the wall energies of Co and Co_5Ce, and indicates a substantial magnetocrystalline anisotropy.

It was found that up to half of the Co in Co_3B could be replaced by Fe while still retaining the orthorhombic structure and easy-axis magnetic symmetry. However, the temperature range of stability of the $(Co, Fe)_3B$ phase decreased with increasing Fe content.

The tetragonal Co_2B phase, in contrast, has easy-plane magnetic symmetry, but easy-axis domain patterns were observed after replacing half of the Co with Fe, i.e., in tetragonal CoFeB, consistent with the observations of Iga.[1]

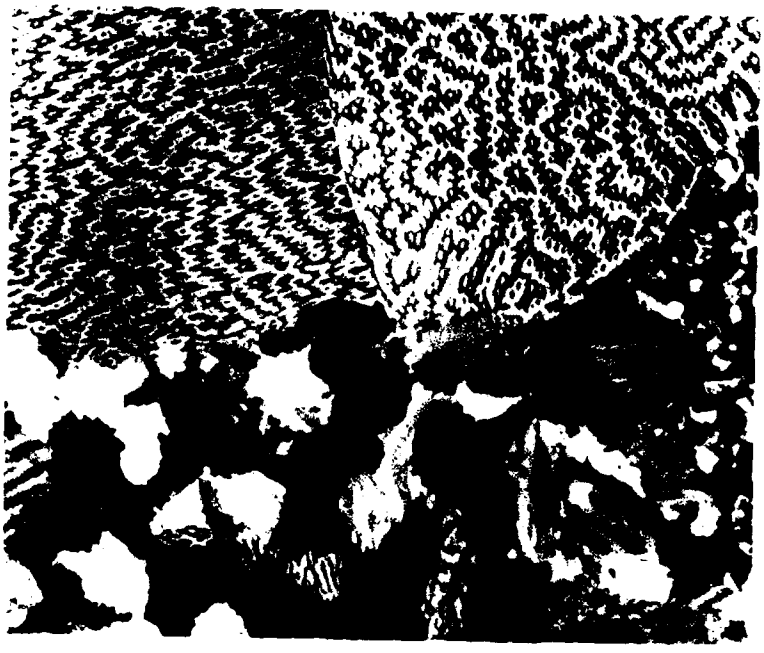

750X
Figure 5 - Domain structure of crystallized Co-24 at.pct. B.

300X
Figure 6 - Domain structure of cast-in Fe_3B crystals in amorphous Fe24 at.pct. B using Bitter technique.

The tetragonal Fe_3B phase showed no Kerr contrast, but domain structure in cast-in Fe_3B crystals in otherwise amorphous Fe - 24 at pct B could be seen with the Bitter technique (Figure 6). These patterns indicate easy axis nearly normal to the surface in the crystal in the lower right.

The Fe_3B phase is metastable and decomposes to Fe_2B plus Fe on heating to elevated temperatures. However, it was found that as little as 2 at pct P can stabilize the tetragonal Fe_3B phase. A crystallized ribbon of Fe - 23 at pct B - 2 at pct P phase contained only tetragonal $Fe_3(B,P)$ at temperatures at least up to 1000°C.

To supplement our studies of crystallized amorphous ribbons, nearly single-phase, large-grained samples of $(Co, Fe)_3B$ and $Fe_3(B,P)$ were prepared by extended annealing of cast alloys and reduced to fine powder for coercivity and anisotropy measurements. Domain structures show that the powders consist primarily of single-crystal particles (Figure 7). Similar powders have been prepared of orthorhombic $Fe_3(B,C)$ and hexagonal Fe_3Sn. All of these phases have substantial Curie temperatures and magnetization and possess anisotropic crystal structures. If subsequent measurements on the various powders reveal any of these phases to have substantial magnetocrystalline anisotropy, that will establish their potential as a permanent-magnet material.

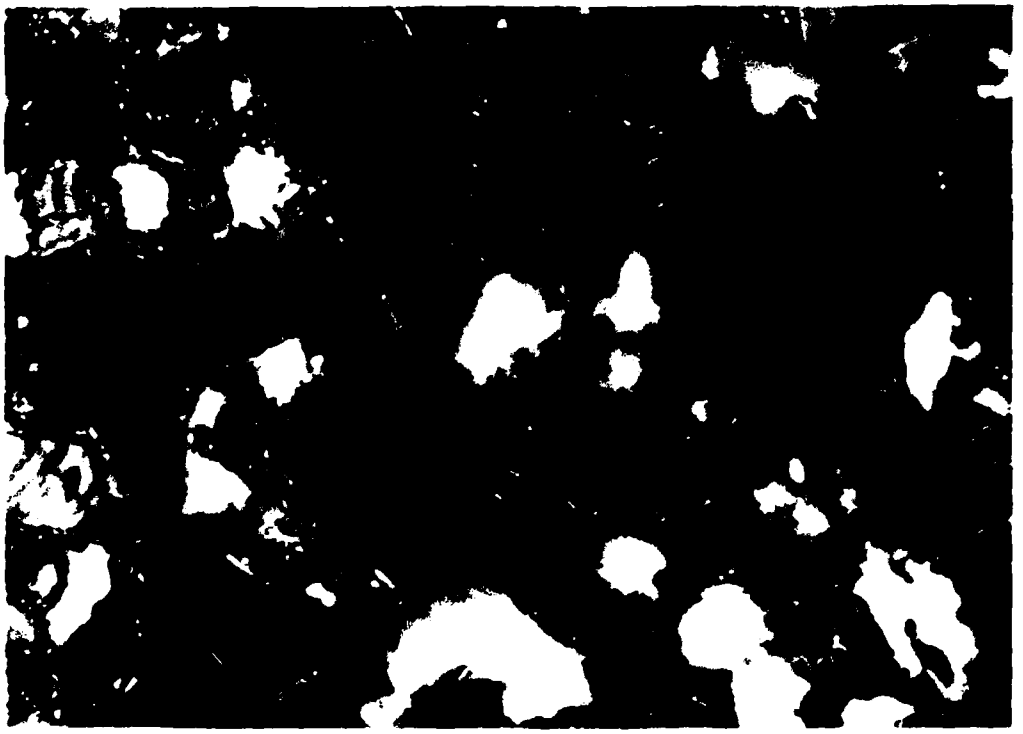

1520X
Figure 7 - Fine powder of $(Co, Fe)_3B$ showing single crystal particles.

Future Directions

The partially transformed nature of the high-coercive-force state appears to be a very important guiding principle in the pursuit of new permanent magnet materials. It is entirely consistent with the idea that a good permanent-magnet material should have a structure that is magnetically as heterogeneous as possible on a very fine scale. Along this line, we have prepared some alloys containing chromium. These can be non-magnetic at room temperature in the amorphous state but strongly magnetic when crystallized, leading to a partially transformed state of maximum magnetic heterogeneity. These alloys are now being investigated. Another possibility is to prepare alloys from systems that exhibit limited liquid solubility, in the hope that more than one amorphous phase may form, as has been seen before.[9] We have prepared alloys containing various amounts of copper. The ingots, while reasonably uniform, show some evidence of having been solidified from a two-liquid melt. Ribbons have been made from these alloys but not yet tested.

The exciting results that have recently been obtained by others with rare earth additions certainly make this an important direction to follow. It is too early to assess the economics, although one must remember that while ten atomic percent rare earth sounds small, it is still 25 weight percent. However, the resulting properties may be worth it, particularly if they can be achieved in the absence of strategic elements such as cobalt. This suggests that the direction of work in this contract can shift from exclusively low-cost materials to those with high performance at moderate cost. Along these lines, preparation methods should not be limited to melt-quenching but include other means of finding interesting and potentially useful materials.

REFERENCES

1. A. Iga, Japan, J. Appl. Phys. 9, 415 (1970)

2. N.C. Koon, C.M. Williams, and B.N. Das, 26th. Annual Conference on Magnetism and Magnetic Materials, November 1980, and private communication

3. A.E. Clark and H.S. Belson, Phys. Rev. B5, 3642 (1972)

4. A.E. Clark, R. Abbundi, and W.R. Gillmor, IEEE Trans. Mag. MAG-14, 542 (1978)

5. J.J. Rhyne, S.J. Pickart, and H.A. Alperin, Phys. Rev. Lett. 29, 1562 (1972)

6. R. Alben, J.J. Becker, and M.C. Chi, J. Appl. Phys. 49, 1653 (1978)

7. A.E. Clark, App. Phys. Lett. 23, 642 (1973)

8. J.J. Croat, A.R. Chraplyvy, and J.F. Herbst, App. Phys. Lett. 37, 962 (1980)

9. J.L. Walter, S.F. Bartram, and I. Mella, Mater. Sci. & Eng. 36, 193 (1978)

PRESENTATIONS AND PUBLICATIONS

The following talks and papers supported by or related to this contract were presented or accepted during the current contract period:

1. JJ Becker, "Crystallized Amorphous Materials"

   Invited talk, part of Symposium on Microstructure and Properties of Magnetic Materials, AIME-ASM-ACS Joint Fall Meeting, October 11-15 1981, Louisville, Kentucky

2. JL Walter, "Effects of Additions on Preparation, Structure, and Crystallization of Some Amorphous Alloys"

   Presented at McGill University, Montreal, Canada, April 8, 1981

   Presented at Naval Research Laboratory, Washington, DC, May 5, 1981

3. JD Livingston, "Magnetic Domains in Cobalt and Iron Borides"

   Presented at 26th Annual Conference on Magnetics and Magnetic Materials, November 11-14, 1980, Dallas, Texas

   J. Appl. Phys. 52, 2506 (1981)

4. JL Walter, JD Livingston, and AM Davis, "Cast-In Crystals in Amorphous Ribbons"

   Mat. Sci. and Eng. 49, 47 (1981)

Abstracts of the talks and the texts of the papers are included in the following section.

CRYSTALLIZED AMORPHOUS METALS*

JJ Becker, General Electric Corporate Research and Development, PO Box 8, Schenectady, NY 12301

Amorphous metals are usually considered as potential soft magnetic materials because of their very low coercive force H_c. However, when they are crystallized H_c increases by orders of magnitude and may reach values that make them potentially useful as permanent magnet materials. These are generally characterized by a magnetically heterogeneous structure on a fine scale and by high magnetocrystalline anisotropy K in one or more phases. Crystallization of amorphous metals sometimes produces phases not otherwise observable, possibly with high K. The highest H_c occurs when the amorphous metal is only partially crystallized. Coercive forces of hundreds of Oe have been produced in materials containing no cobalt or rare earths and thousands of Oe have been attained with rare earths. The present situation will be summarized, including composition effects, current-pulse crystallization and resistivity monitoring, magnetic analysis, and other experimental methods.

*Supported in part by the Office of Naval Research

EFFECTS OF ADDITIONS ON PREPARATION, CRYSTALLIZATION, AND STRUCTURE OF SOME AMORPHOUS ALLOYS*

JL Walter, General Electric Corporate Research and Development, PO Box 8, Schenectady, NY 12301

Elemental additions to transition metal-metalloid binary amorphous alloys often make it easier to prepare completely amorphous alloys. These same additions may also have profound effects on the temperatures of crystal nucleation and growth. It might be expected that these additions would also affect the amorphous structure.

This talk examines effects of various additions to the Fe-B and Co-B binary alloy systems in terms of ability to prepare amorphous ribbons free of cast-in crystals. The characteristics of the cast-in crystals versus those formed by heating to crystallization are described. The effects of additions on crystallization are also examined. It is shown that the change of crystallization temperature as a function of amount of third element added to binary Fe-B alloys is directly related to the difference in atom radii between the iron atom and the addition atom for ten different elements.

Changes in structure as a function of additions are inferred from microhardness measurements, Mossbauer spectroscopy, and measurements of the rate of increase of viscosity for, for example, the $Fe_{82-x}B_{18}Si_x$ alloy system. It is observed that while the activation energy for crystallization, the crystallization temperature, and the microhardness increase with increasing Si content, there is no change in the Mossbauer spectra nor does the activation energy for the rate of increase of viscosity change with increasing Si. These and other results are related to structures of the amorphous alloys.

*Supported in part by the Office of Naval Research

GENERAL ELECTRIC

General Electric Company
Corporate Research and Development
Schenectady, New York

TECHNICAL INFORMATION SERIES

AUTHOR	SUBJECT	NO / DATE
Walter, JL Livingston, JD Davis, AM*	amorphous metals	80CRD255 November 1980
TITLE		GE CLASS / NO PAGES
Cast-In Crystals in Amorphous Ribbons		1 15
ORIGINATING COMPONENT		CORPORATE RESEARCH AND DEVELOPMENT SCHENECTADY, N.Y.
Metallurgy Laboratory		

SUMMARY

Cast-in crystals have been observed in amorphous alloy ribbons of Co-B, Fe-B, Ni-B, FeNi-B, and FeCo-B prepared by the chill-block casting technique. Their presence was determined by optical microscopy, microradiograhy, x-ray diffraction, scanning and transmission electron microscopy, and Bitter and Kerr domain observation techniques. The cast-in crystals are often very large, indicating growth velocities greater than 1 cm/s and growth temperatures greater than 1000 °C. Most of the crystals are of the expected stable phase but in the Fe-B series, the cast-in crystals are of the metastable bc tetragonal Fe_3B phase.

*Inorganic Materials and Structures Laboratory

KEY WORDS

amorphous metals, amorphous ribbons, crystals, chill cast ribbons, cast-in crystals

INFORMATION PREPARED FOR _____

Additional Hard or Microfiche Copies Available From

Technical Information Exchange
Bldg. 81 Room A133, Schenectady, N.Y., 12345

CAST-IN CRYSTALS IN AMORPHOUS RIBBONS

J.L. Walter, J.D. Livingston, and A.M. Davis

INTRODUCTION

Amorphous alloy ribbons are commonly prepared by the chill-block casting technique, in which a stream of molten alloy is ejected onto a rapidly moving chill surface. Alloy ribbons that are partly or fully crystalline can also be prepared by this technique, either directly from casting or by heating an initially amorphous ribbon. Such ribbons may exhibit unusual physical properties, because the high quenching rates of chill-block casting can produce microstructures and, in some cases, metastable phases not attainable by ordinary casting techniques.

Although the crystallization of amorphous alloys by heating has received considerable attention, there has been little discussion of the cast-in crystals that sometimes occur in amorphous ribbons. Whether they are a desired or an undesired part of the final product, it is important to characterize these crystals and understand their formation.

We report here observations on cast-in crystals in a number of transition metal-boron alloys. Since cast-in crystals in small volume fractions often escape detection by conventional x-ray techniques, we emphasize a variety of supplementary experimental techniques that have been found useful.

EXPERIMENTAL PROCEDURE

Ingots of Co-B, Fe-B, Ni-B, FeNi-B, and FeCo-B were prepared by melting and chill casting under argon in an induction furnace. The starting materials were vacuum-melted cobalt, vacuum-melted electrolytic iron, 270 nickel, and 99.8% crystal boron. The ingots were then crushed and used as starting materials in the preparation of alloy ribbons by chill block casting.[1] A copper drum of 10 or 15 cm diameter was used, with a surface speed of about 30 m/s. The resulting ribbon was about 27 μm thick by 1-2 mm wide.

Ribbons were routinely examined by optical microscopy and x-ray diffraction, including both Debye-Scherrer and pinhole transmission diffraction. The latter technique, while covering a similar area of sample, is more sensitive than the Debye-Scherrer technique in detecting cast-in crystals. X-ray diffraction analysis of residues after etching also proved useful. Selected samples were examined by transmission electron microscopy (TEM), scanning electron microscopy, microradiography, and Bitter and Kerr domain-observation techniques.

EXPERIMENTAL RESULTS

Co-B

In some cases, cast-in crystals as large as 100 μm are observed, as in the $Co_{74}B_{26}$ ribbon shown in Figure 1.* Such crystals generally have depressed centers on the air side of the ribbon, suggesting that crystal growth terminated on this surface while the ribbon was still liquid. Such crystals are also usually associated with depressed areas on the drum side of the ribbon, generally much larger than the crystals themselves. These areas result from entrapped air pockets at the melt-drum interface. The resulting reduction in local quenching rate apparently contributes to the nucleation and growth of cast-in crystals.

Debye-Scherrer analysis of this and other Co-B ribbons failed to reveal the presence of cast-in crystals in amounts less than about 5% by volume, although they could be revealed both by optical microscopy and by measurements of the temperature coefficient of resistivity.[2] The crystals were identified by Debye-Scherrer analysis of the residue remaining after electrolytically thinning the ribbon in 7% HCl/methanol, which preferentially dissolves the amorphous matrix. Such residue analysis for a series of Co-B ribbons identified the cast-in crystals as tetragonal Co_2B for $Co_{70}B_{30}$ and $Co_{72}B_{28}$, orthorhombic Co_3B for $Co_{75}B_{25}$, $Co_{77}B_{23}$, and $Co_{80}B_{20}$, and as a mixture of Co_3B and fcc Co for $Co_{84}B_{16}$.

Contact microradiography was applied to each of the above alloys after etching to remove some of the amorphous matrix and expose the crystals. In this technique, a photographic emulsion is placed in direct contact with the ribbon surface, and an image is obtained by differential absorption of the x-rays. Microradiographs of as-cast $Co_{80}B_{20}$ and $Co_{70}B_{30}$ ribbons are shown in Figure 2. The light regions are the crystals.

* All figures appear at the end of this report.

Manuscript received October 14, 1980

The difference in magnetic properties between cast-in crystals and the amorphous matrix can also be useful in characterizing such crystals. Orthorhombic Co_3B has a strongly preferred crystallographic axis of magnetization. When this axis has a component normal to the surface, the emerging fields strongly attract the ferrofluid used in the Bitter domain-observation technique as seen in Figure 3a, showing crystals in $Co_{76}B_{24}$ ribbon. On a mechanically polished surface, these emerging fields also result in strong domain contrast in polarized light by the polar Kerr effect (Figure 3b). The cast-in Co_2B crystals in the higher-boron ribbons neither attract ferrofluid nor show Kerr contrast. This results from the easy-plane magnetic symmetry of Co_2B, which allows the magnetization to remain parallel to the specimen surface. Domain patterns such as those in Figures 3a and 3b are determined by the orientation of the magnetic easy axis of Co_3B. Thus the Bitter and Kerr techniques can be helpful not only in identifying the phases of cast-in crystals, but also in determining their orientation.

Transmission electron microscopy of as-cast $Co_{78}B_{22}$ ribbon reveals Co_3B crystals with widely varying microstructures. Some contain fault-like features (Figure 4a), some cellular features (Figure 4b), and some an extensive, ultrafine structure (Figure 4c). The microstructure of Co_3B crystals in $Co_{78}B_{22}$ is again different, both for cast-in crystals (Figures 5a,b) and for crystals formed on heating to 709 K (Figure 5c). The diffraction pattern of the crystals formed on heating (Figure 5c) shows highly faulted crystals, and these crystals are reminiscent of Fe_3B crystals formed by heating $Fe_{80}B_{20}$ and $Fe_{50}Ni_{30}B_{20}$ ribbons.[3]

Heating of amorphous ribbons containing cast-in crystals leads both to the formation of fine crystals from the amorphous phase and to the further growth of the large cast-in crystals (Figure 6a). This layer of new growth can also be seen by microradiography (Figure 6b) and scanning electron microscopy (Figure 6c) of ribbons in which the matrix has been partly etched away.

Fe-B

As reported elsewhere,[4] Fe-B ribbons with less than 14% or more than 21% boron were found to contain cast-in crystals. The low-boron ribbons contained round alpha-iron crystals quite different in morphology from the dendritic alpha-iron crystals produced on heating these hypoeutectic alloys.[5] The high-boron ribbons contained cast-in crystals of metastable tetragonal Fe_3B, which attracted ferrofluid strongly (Figure 7a). Use of dark-field microscopy reveals magnetic domain patterns in the surrounding amorphous matrix (Figure 7b). Interpretation of these patterns[6] indicates that the matrix is under compression in the direction of the c-axis of the Fe_3B crystal, and under tension in directions normal to the c-axis. These stresses presumably result from anisotropic differential thermal contraction between matrix and crystal during cooling, the crystal a-axis contracting more, and the c-axis less, than the matrix.

By transmission electron microscopy, the cast-in tetragonal Fe_3B crystals are usually nearly featureless,[7] although some heavily structured, finer Fe_3B crystals are found imbedded within the larger crystals (Figure 8a). These latter crystals decompose to the equilibrium Fe_2B and alpha-iron phases on heating to 773 K (Figure 8b), whereas the larger, featureless crystals do not decompose until much higher temperatures.

Fe_3B crystals formed from the amorphous phase in $Fe_{75}B_{25}$ and $Fe_{76}B_{24}$ by heating also appear featureless. Heating $Fe_{84}B_{16}$ produces primary alpha-iron particles and featureless Fe_3B.[5] However, heating $Fe_{80}B_{20}$ produced only Fe_3B crystals with an ultrafine but strong columnar microstructure.[3]

Fe-Ni-B

Transmission electron microscopy of as-cast $Fe_{43}Ni_{43}B_{14}$ and $Fe_{39}Ni_{39}B_{22}$ ribbons indicate that most cast-in crystals have the fcc $(Fe,Ni)_{23}B_6$ structure (isostructural with $Cr_{23}C_6$). Some crystals are essentially featureless while others, sometimes even adjacent crystals, appear highly faulted.[7] In addition to very large cast-in crystals, as discussed above for Co-B and Fe-B, there were also numerous finer crystals (Figure 9). An area originally thought to be amorphous (Figure 10a) was found, by diffraction pattern (Figure 10b) and dark-field microscopy (Figure 10c) to be microcrystalline, with an average grain size of about 250 Å.

FeCo-B

Ribbons of $Fe_{38}Co_{38}B_{24}$ contain cast-in crystals of orthorhombic $(FeCo)_3B$ with no microstructural features. However, ribbons of $Fe_{44}Co_{44}B_{12}$ have cast-in crystals, identified as $(FeCo)_3B$ by diffraction analysis, that contain a pronounced substructure. One such crystal appears in Figure 11, in which the diffraction pattern indicates a spread of about 12° about the [322] normal to this crystal.

Ni-B

In the alloys discussed above, most cast-in crystals, both large and small, appear relatively unfaceted. In contrast, some of the cast-in crystals in $Ni_{62}B_{38}$ ribbon are hexagonal in form and contain a dendritic substructure, much like a snowflake (Figure 12). These crystals have been identified by x-ray diffraction as orthorhombic Ni_4B_3.

DISCUSSION

For each alloy and crystallization mode, the rate of crystallization will go through a maximum with decreasing temperature, producing the familiar C-curve.[8] When crystallization occurs on heating an amorphous alloy, it occurs on the lower portion of this C-curve. However, most cast-in crystals grew on the upper portion of the C-curve, at much higher temperatures and velocities than the crystals formed on heating. Estimating from known cooling rates,[1] large cast-in Fe_3B crystals such as those in Figure 7 grew in times less than 10^{-2} s, hence at growth velocities greater than 1 cm/s. By extrapolating data from Herold and Koster,[9] for Fe_3B growth at lower temperatures, such velocities indicate that these crystals grew at temperatures over 1000 °C. The same is probably true for the large ($>10\ \mu m$) cast-in crystals observed in the other alloys studied. Their association with air pockets on the drum side of the ribbon indicates their formation was aided by a local lowering of the cooling rate. However, only a small fraction of the air pockets had associated cast-in crystals, indicating that crystal formation was limited by a shortage of nucleation sites.

The much smaller cast-in crystals sometimes seen, such as those in Figures 9 or 10, probably formed at much lower temperatures, on the lower portion of the C-curve. The high initial cooling rates characteristic of chill block casting are maintained only while the ribbon maintains contact with the drum. Even when such initial cooling is sufficiently rapid to avoid the nose of the C-curve, the much slower cooling that occurs after leaving the drum can allow crystallization to occur at lower temperatures.

Herold and Koster[9] have distinguished between three different crystallization modes in alloys such as these: polymorphous crystallization (single-phase growth with no composition change), primary crystallization (single-phase growth with rejection of solute), and eutectic crystallization (simultaneous two-phase growth). Most of the cast-in crystals are probably examples of polymorphous crystallization, the crystallization mode that requires the least diffusion.

In most of the alloys studied, the phase of the cast-in crystals is present in the equilibrium phase diagram, although it often formed well off equilibrium stoichiometry. The exception is Fe-B, where the tetragonal Fe_3B phase is a metastable phase. This phase forms on crystallization of heated amorphous ribbons,[3,5] but on further heating to 600 °C or above, decomposes to the equilibrium Fe_2B + Fe phases.[9] It is interesting that the cast-in crystals grow with the metastable Fe_3B structure at temperatures well in excess of these decomposition temperatures. Apparently the short times involved favored polymorphous crystallization, much as lowered diffusion rates favor this mode at lower temperatures.

The presence of Fe_3B crystals in the cast ribbon might be expected since it appears that the chemical short range order of the amorphous $Fe_{75}B_{25}$ is similar to the short range order of crystalline Fe_3B.[5,10] It has been suggested that this unique ordering may extend to the Fe-B melt[5] which could account for the preference for the cast-in metastable Fe_3B crystals over the stable Fe_2B crystals which grow from the melt at lower cooling rates.[4]

Since cast-in crystals and crystals formed on heating grow under much different conditions, it is not surprising that their microstructures, as observed by TEM, are often different. The high growth rates themselves may sometimes lead to faulted structures, but faults may also be caused by off-stoichiometric compositions. Slight deviations from stoichiometry can be accommodated by faults that do not preserve composition, such as crystallographic shear planes.[11] It may sometimes be difficult to distinguish between such faults and fine second-phase regions, i.e., fine eutectic crystallization. Some of the highly structured crystals often seen, such as those in Figures 5 and 11 and the Fe_3B crystals in heated $Fe_{80}B_{20}$ ribbon,[3] may in fact be two-phase on a very fine scale, even though the minority metallic phase was not detected in diffraction patterns.

The small structured Fe_3B crystals seen in Figure 8a may contain such fine Fe inclusions, which would provide easy nucleation sites for the decomposition to the equilibrium Fe_2B and Fe phases (Figure 8b).

Finally, we note the utility of a broad variety of experimental techniques in detecting and characterizing cast-in crystals. X-ray diffraction of ribbons or etching residue, optical microscopy, transmission

and scanning electron microscopy, microradiography, and resistivity measurements all may contribute helpful information. Where the phases formed are ferromagnetic, Bitter and Kerr domain-observation techniques are also useful.

ACKNOWLEDGMENTS

Optical microscopy was performed by C.R. Rodd and transmission electron microscopy by E.F. Koch of the Inorganic Materials and Structures Laboratory

REFERENCES

1. J.L. Walter, *Rapidly Quenched Metals, III, V.I.*, The Metals Society, London, 1978, p. 30.
2. A. Mogro-Campero and J.L. Walter, to be published, also General Electric TIS Report 80CRD073.
3. J.L. Walter, S.F. Bartram, and R.R. Russell, *Metall. Trans. 9A* (1978) 803.
4. J.L. Walter, to be published in *J. Non-Crys. Solids.*
5. J.L. Walter, S.F. Bartram, and I. Mella, *Mater. Sci Eng. 36* (1978) 193.
6. J.D. Livingston, *Phys. Status Solidi A 56* (1979) 637.
7. J.L. Walter, Proceedings of the 2nd International Conference on Rapid Solidification Processing, Virginia, March 1980.
8. H.A. Davies, *Phys. Chem. Glasses 17* (1976) 159.
9. U. Herold and U. Koster, *Rapidly Quenched Metals, III*, The Metals Society, London, VI (1978) p. 281. Also, U. Koster and U. Herold, to be published in *Metallic Glasses*, Springer, 1980.
10. I. Vincze, D.S. Boudreaux, and M. Tegze, *Phys. Rev. B 19* (1979) 4896.
11. J.S. Anderson, *J. Chem. Soc., Dalton Trans. 10* (1973) 1107.

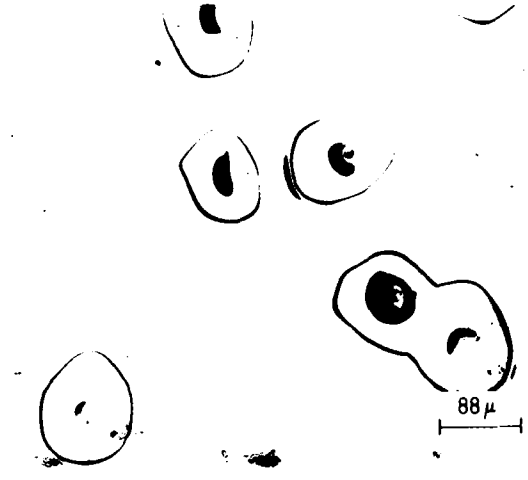

Figure 1. Crystals on the surface of $Co_{74}B_{26}$ ribbon.

(a)

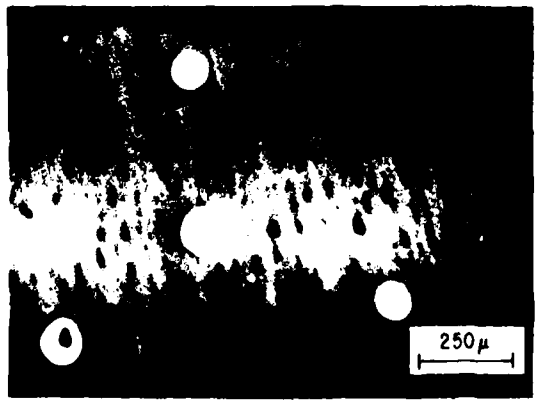

(b)

Figure 2. (a) Microradiograph of crystals in $Co_{80}B_{20}$ ribbon, and (b) microradiograph of crystals in $Co_{70}B_{30}$ ribbon.

(a) (b)

Figure 3. (a) Magnetic domains in crystals in $Co_{76}B_{24}$ ribbon using the Bitter technique, and (b) magnetic domains revealed by the Kerr technique in crystals in $Co_{76}B_{24}$ ribbon.

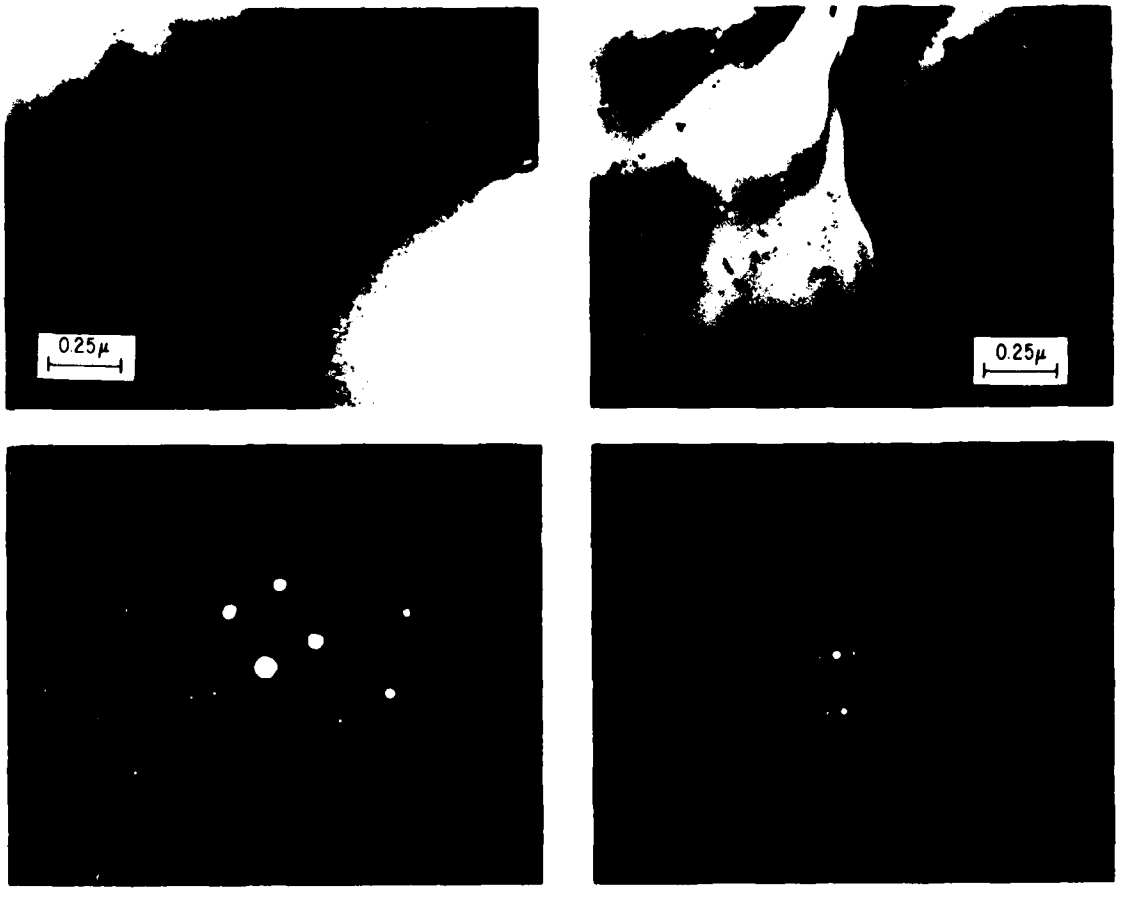

(a) (b)

Figure 4. Transmission electron micrographs and selected area diffraction patterns of Co_3B crystals in $Co_{75}B_{25}$ ribbon; (a) with fault-like features, (b) with cell-like features.

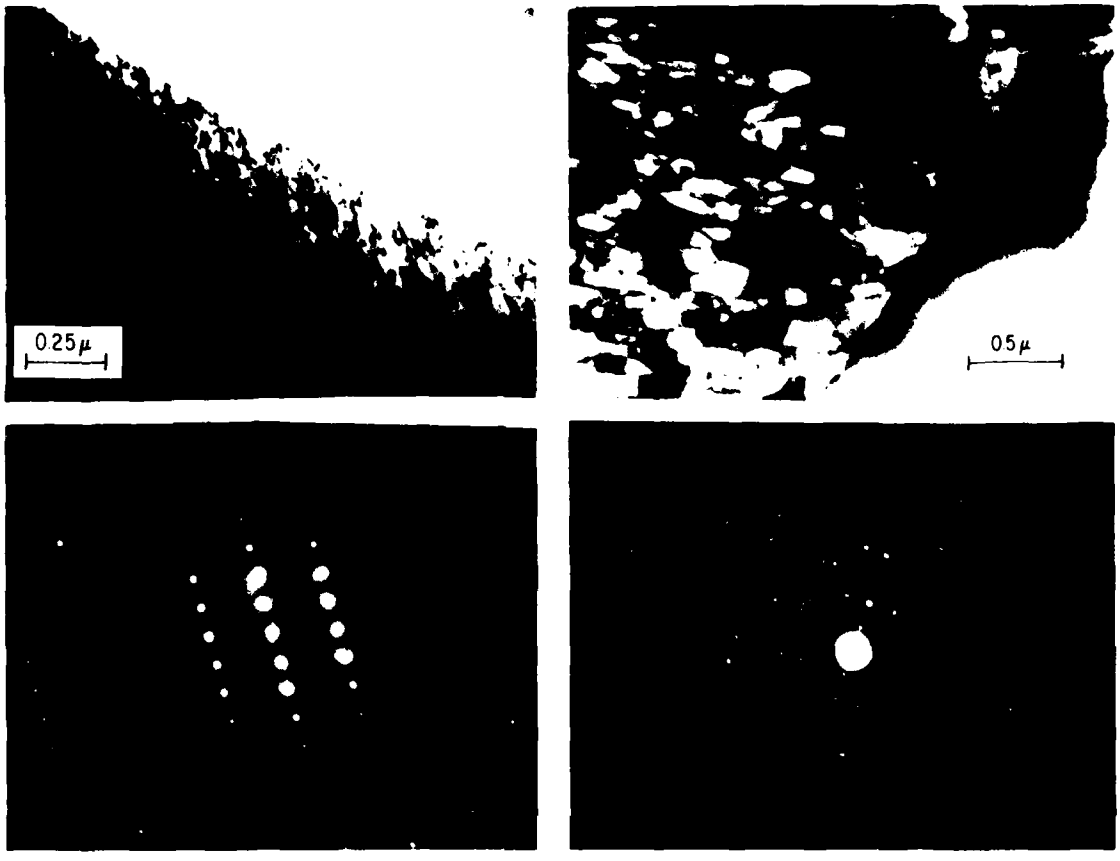

(c)

Figure 4 (continued). (c) With ultrafine structure.

(a)

Figure 5. TEM and electron diffraction patterns Co_3B crystals; (a) in cast $Co_{78}B_{22}$ ribbon.

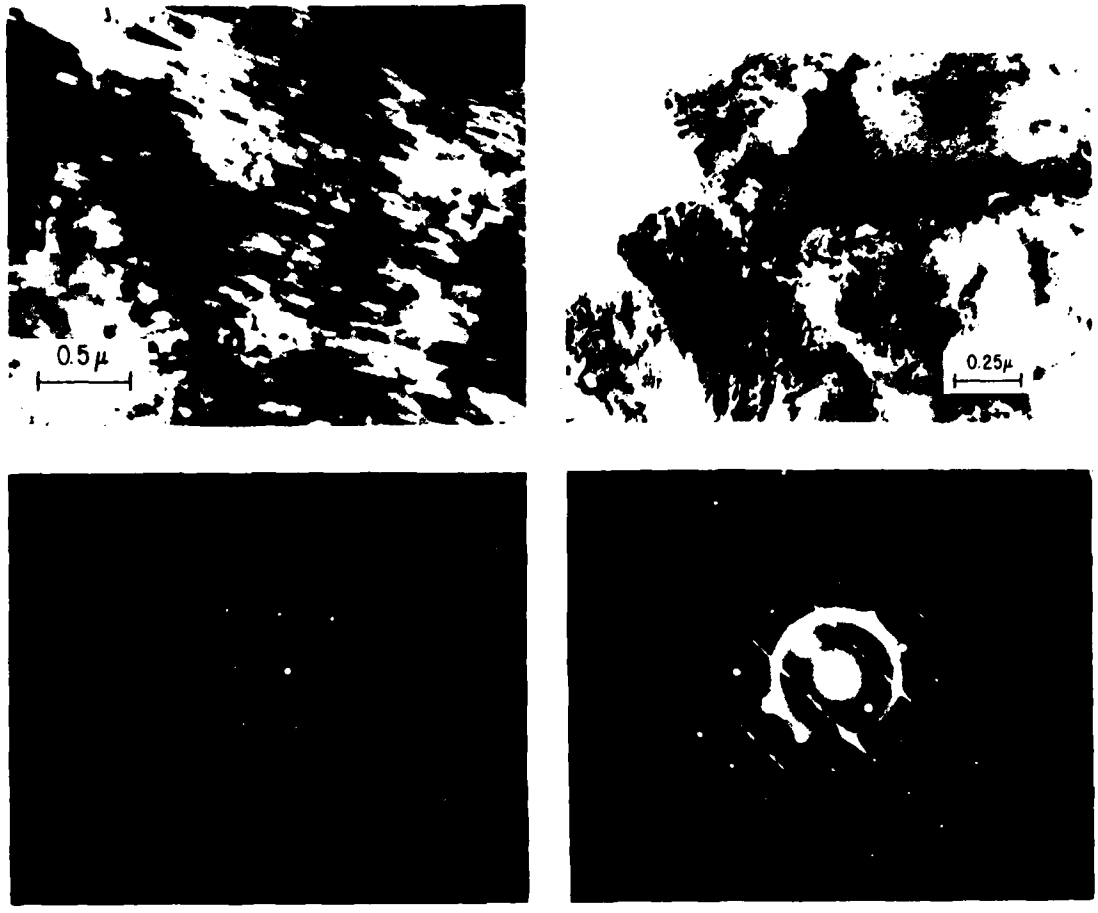

(b) (c)

Figure 5 (continued). (b) In cast $Co_{78}B_{22}$ ribbon, and (c) in ribbon heated to 709 K and quenched.

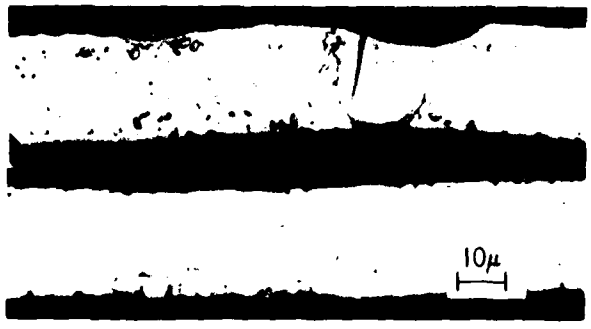

(a)

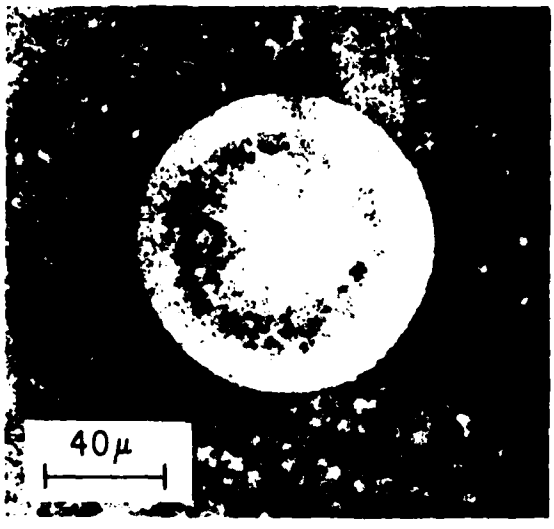

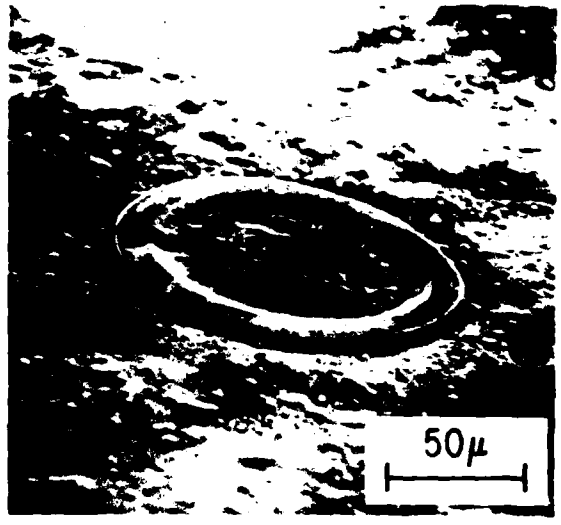

(b) (c)

Figure 6. (a) Optical micrographs of cast-in crystals in longitudinal sections of $Co_{80}B_{20}$ ribbon showing growth caused by heating, (b) microradiograph of crystal in $Co_{70}B_{30}$ ribbon heated to 735 K and quenched, and (c) scanning electron micrograph of crystal in $Co_{70}B_{30}$ ribbon heated to 735 K and quenched.

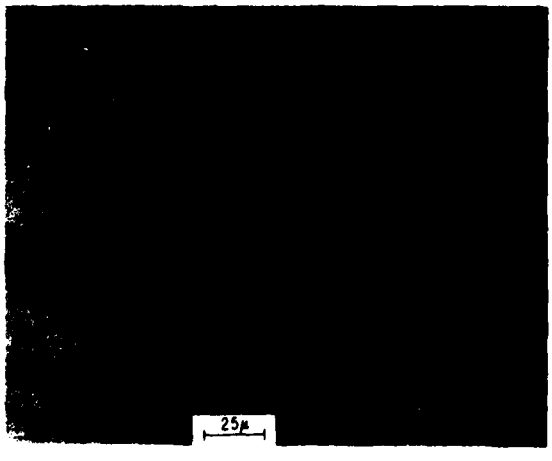

(a) (b)

Figure 7. Magnetic domain in $Fe_{76}B_{24}$ ribbon; (a) in crystals revealed by the Bitter technique, and (b) in adjacent amorphous matrix revealed by dark-field microscopy.

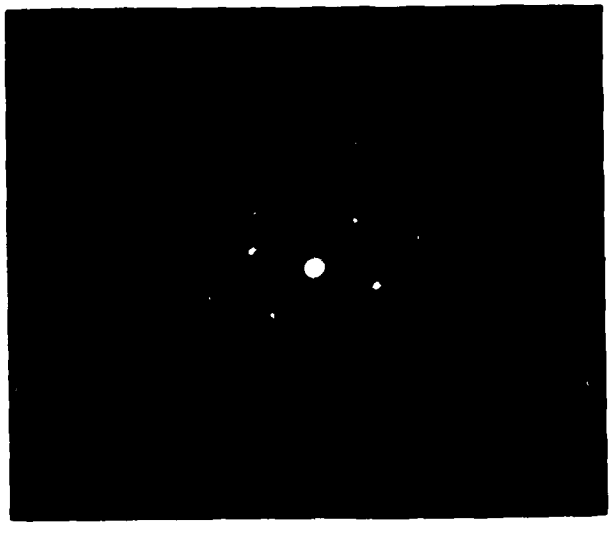

Figure 8. (a) TEM of Fe_3B crystals (featureless and microstructured) in cast $Fe_{75}B_{25}$.

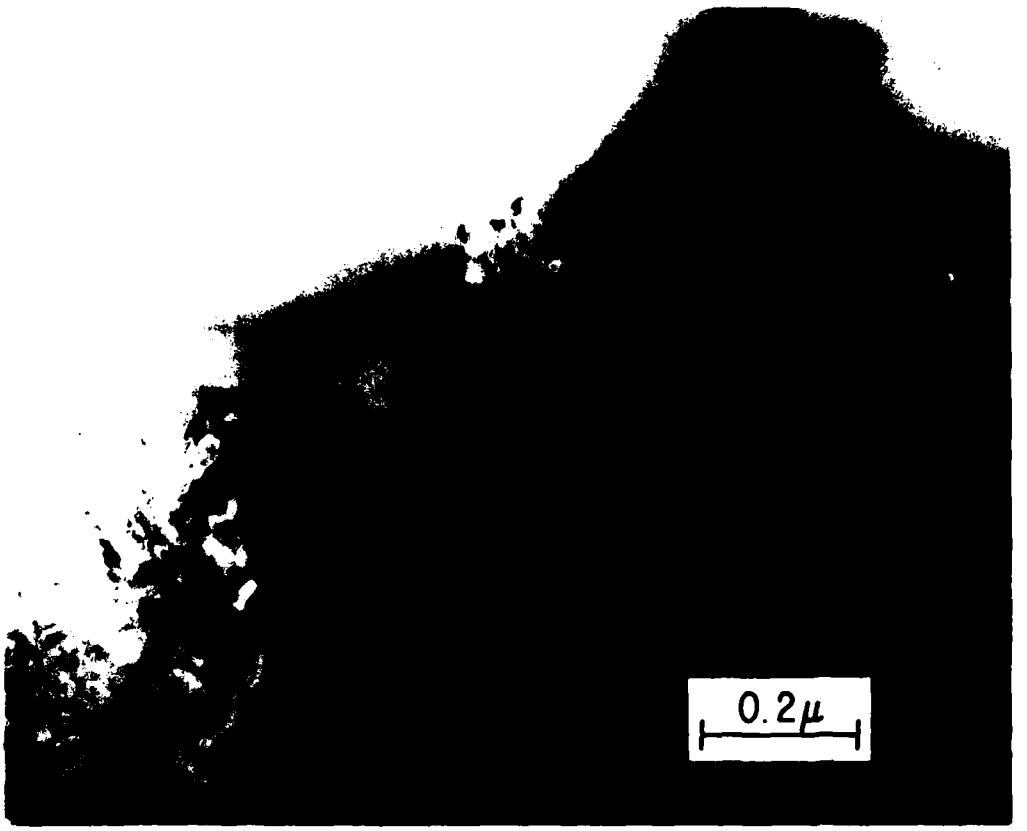

Figure 8 (continued). (b) Featureless and decomposed (Fe_2B + alpha-iron) crystals in $Fe_{75}B_{25}$ heated to 773 K.

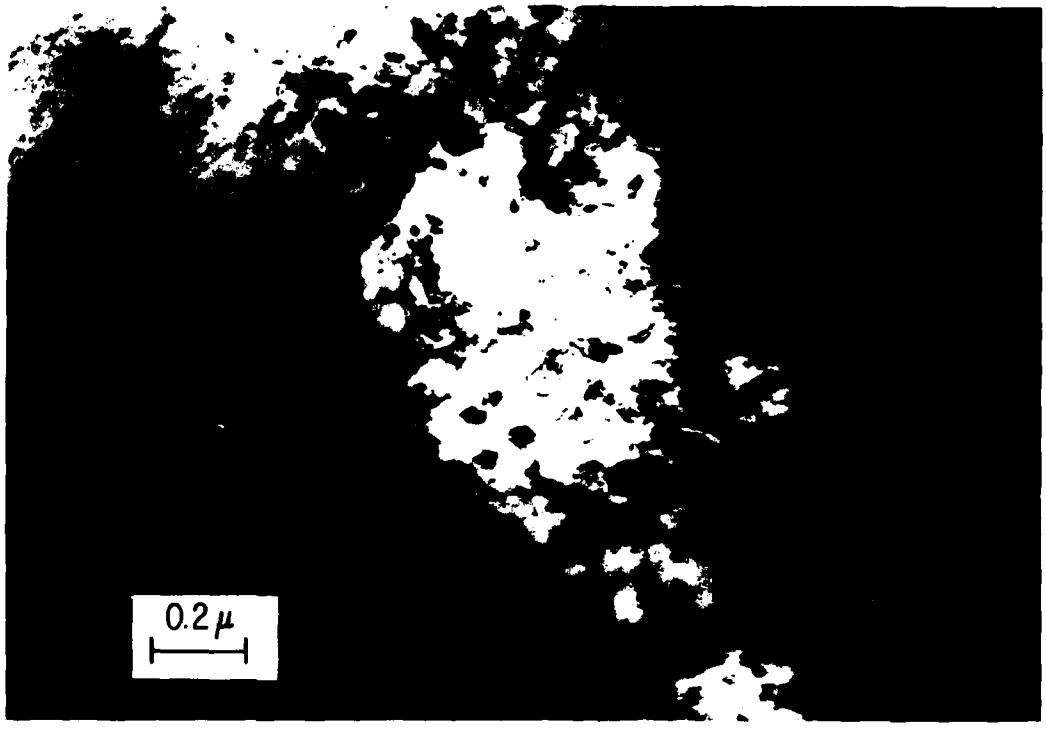

(a)

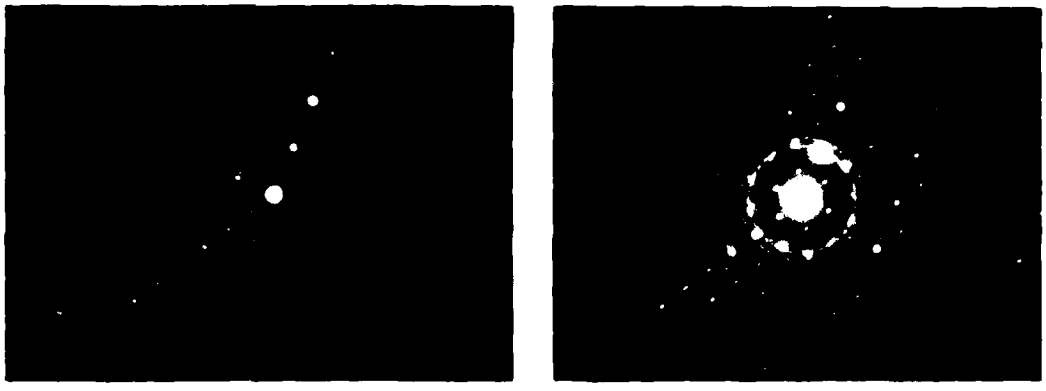

(b) (c)

Figure 9. (a) TEM of large (left-hand side) and fine $(Fe, Ni)_{23}B_6$ crystals in $Fe_{43}Ni_{43}B_{14}$ ribbon, (b) electron diffraction pattern of large crystal area, and (c) electron diffraction pattern of fine crystal area.

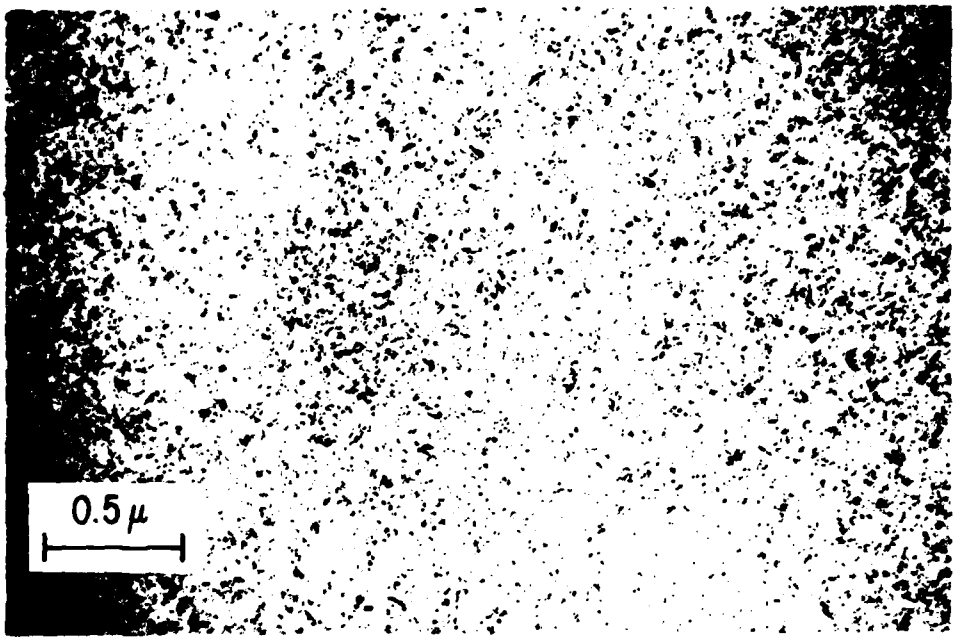

(a)

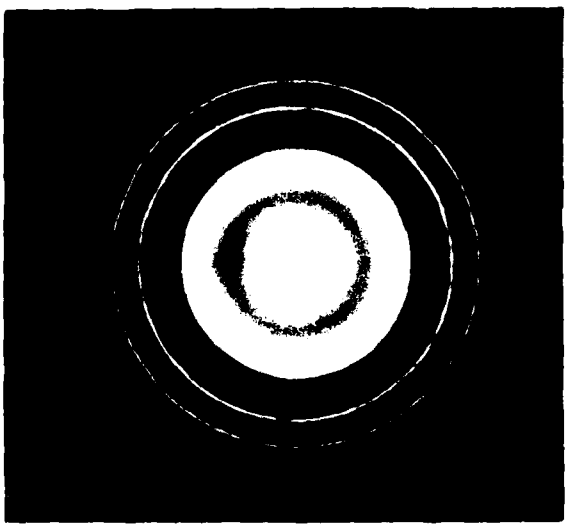

(b)

Figure 10. (a) TEM of $Fe_{43}Ni_{43}B_{14}$ ribbon containing crystals of average size 250 Å. (b) electron diffraction of area (a).

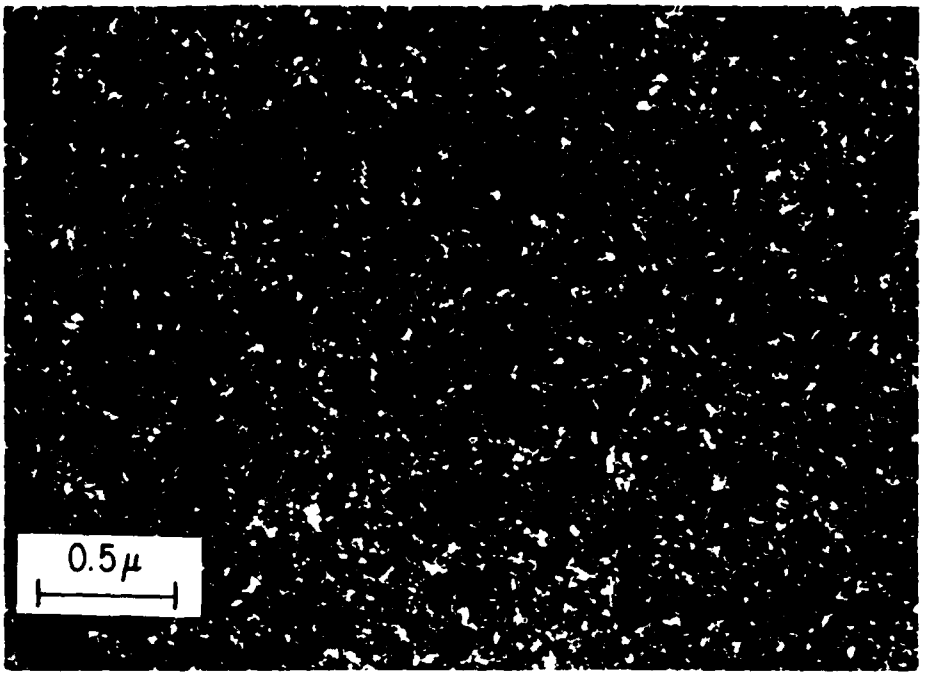

(c)

Figure 10 (continued). (c) Dark field of area in (a).

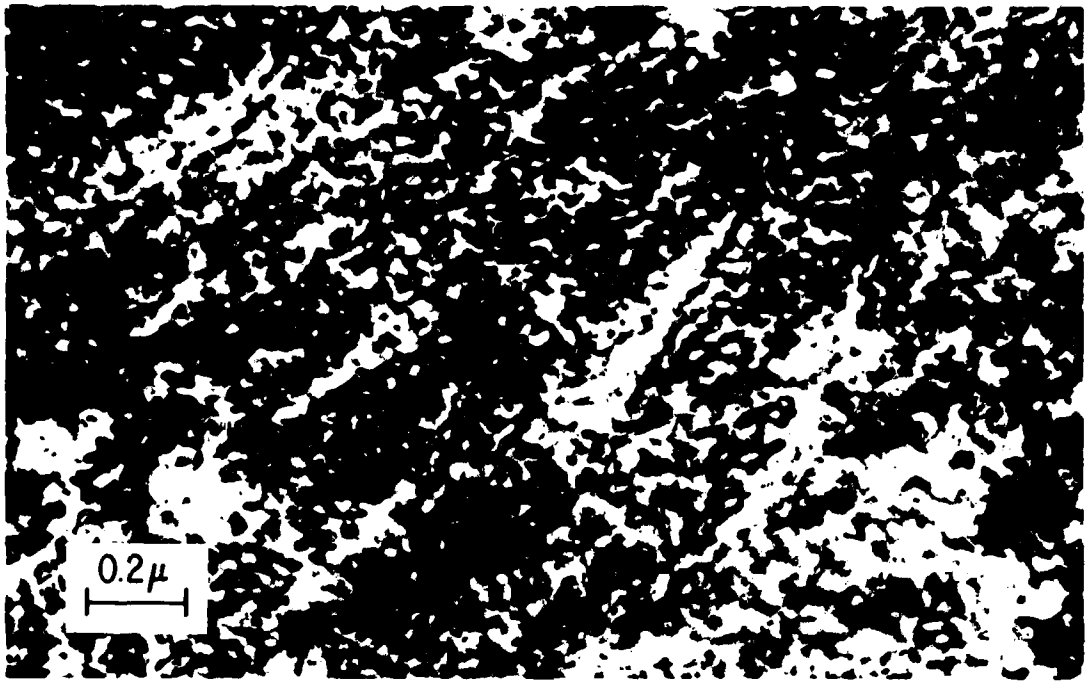

(a)

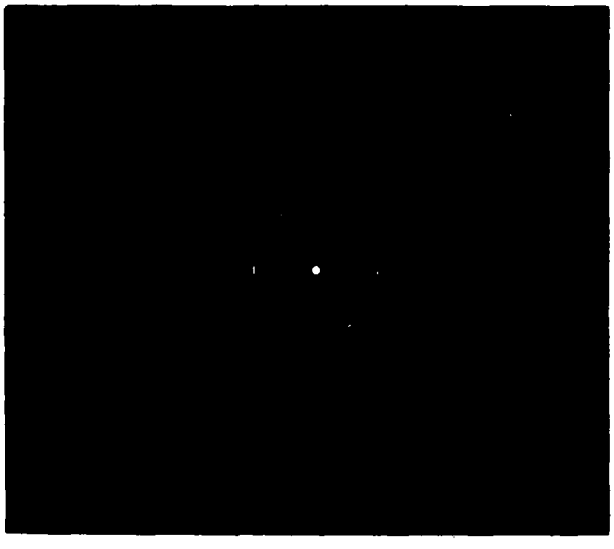

(b)

Figure 11. (a) TEM of large crystal with substructure in $Fe_{44}Co_{44}B_{12}$ ribbon, and (b) diffraction pattern of area in (a).

Figure 12. Optical micrograph of crystals on surface of $Ni_{62}B_{38}$ ribbon.

GENERAL ELECTRIC

General Electric Company
Corporate Research and Development
Schenectady, New York

TECHNICAL INFORMATION SERIES

AUTHOR	SUBJECT	NO.
Livingston, JD	magnetic materials	80CRD256
		DATE November 1980
TITLE		GE CLASS
Magnetic Domains in Cobalt and Iron Borides		1
		NO. PAGES 4
ORIGINATING COMPONENT		
Metallurgy Laboratory		CORPORATE RESEARCH AND DEVELOPMENT SCHENECTADY, N.Y.

SUMMARY

Using Kerr and Bitter techniques, magnetic domain patterns have been studied in various cobalt, iron, and cobalt-iron borides prepared by chill casting, directional solidification, and melt-spinning. Magnetic symmetries and metallurgical stability of the phases are discussed.

KEY WORDS

magnetic domains, magnetic anisotropy, metallography

INFORMATION PREPARED FOR _____

_____

Additional Hard or Microfiche Copies Available From

Technical Information Exchange
Bldg. 81 Room A133, Schenectady, N.Y., 12345

MAGNETIC DOMAINS IN COBALT AND IRON BORIDES

J.D. Livingston

INTRODUCTION

Crystallization of amorphous Co-B or Fe-B alloys generally leads to the formation of orthorhombic Co_3B or tetragonal Fe_3B phases.[1] We have studied magnetic-domain patterns in these and related ternary phases, produced in various ways, as part of a general program examining the magnetic properties of crystallized amorphous alloys. Domain studies can be useful both in microstructural analysis and in identification of magnetic symmetries.

EXPERIMENTAL

Various Co-B, Co-Fe-B, Fe-B, and Fe-B-P alloys were prepared by melting and chill casting under argon in an induction furnace. Portions of the ingots were crushed and used as starting material for chill-block melt-spinning.[2] This process produced largely amorphous ribbons, about 27 μm thick and 1-2 mm wide. Selected alloys were also produced by directional solidification of 1.9-cm-diameter ingots, at a rate of 0.64 cm/hr under a temperature gradient of 170 °C/cm. Various annealing experiments were done under argon or in evacuated quartz tubes. Portions of the samples were crushed to powder and analyzed by Debye-Scherrer technique. Magnetic domains were observed using polarized light in normal incidence (the polar Kerr technique) or by applying ferrofluid to freshly polished or as-cast surfaces (the Bitter technique).[3]

OBSERVATIONS

The orthorhombic Co_3B phase is stable between 1125 °C, where it forms by peritectic reaction between Co_2B and the Co-rich melt, and 845 °C, below which it decomposes (sluggishly) to $Co+Co_2B$ by eutectoid reaction.[4] Its peritectic formation is clear from the microstructure of chill-cast ingots of Co-25 at.% B (Figure 1a). The Co_3B phase appears as a reaction layer around the faceted Co_2B dendrites, and is in turn surrounded by $Co+Co_3B$ eutectic. Chill-cast ingots in which one quarter or one-half of the Co is replaced by Fe show similar microstructures. However, annealing these Co-B and Co-Fe-B ingots for three days at 1030 °C produces essentially single-phase orthorhombic Co_3B or $(Co,Fe)_3B$ (Figure 1b). The domain structure seen

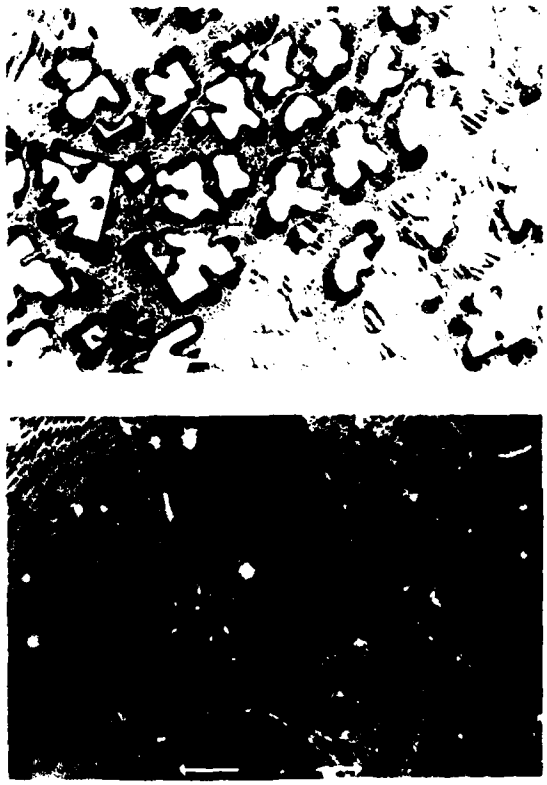

Figure 1. (a) Chill casting of Co-25 at.% B, (b) annealed casting of $(Co_{.75}Fe_{.25})_3B$. Arrows in these and subsequent figures indicate 50 μm.

by the Kerr effect in Figure 1b (and in the Co_3B phase in Figure 1a) resembles that seen in Co and other materials with substantial magnetic anisotropy and a single, easy (low energy) direction.[3]

Nearly single-phase Co_3B can also be produced by directional solidification of Co-25 at.% B (Figure 2a), in which the formation of a Co-rich liquid layer at the solid-liquid interface allows direct formation of Co_3B from the melt. However, directional solidification of the Fe-substituted alloys leads only to peritectic multiphase microstructures (Figures 2b and 2c), probably because the Fe lowers the formation temperature of the Co_3B phase. With

Manuscript received October 14, 1980

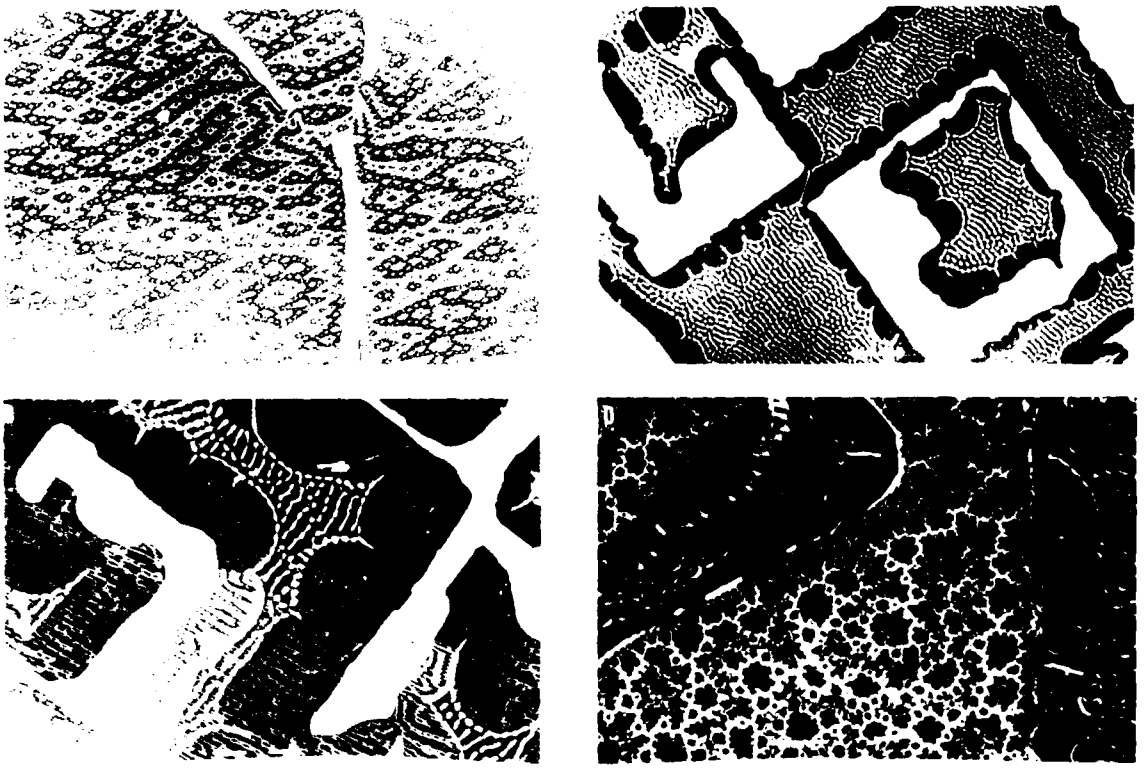

Figure 2. Transverse sections of directionally solidified ingots; (a) Co-25 at.% B, (b) Co-18.8 Fe-25 B, (c) Co-37.5 Fe-25 B, (d)Co-37.5 Fe-25 B with Bitter solution, dark field.

increasing Fe, the reacted layer of $(Co,Fe)_3B$ decreases in thickness, while the volume fractions of eutectic and of $(Co,Fe)_2B$ dendrites increase. Metallographic evidence of eutectoid decomposition of the $(Co,Fe)_3B$ phase in some regions of the higher Fe alloys suggests that Fe also raises the eutectoid temperature.

The substitution of Fe for one-half of the Co produces faint domain contrast by the Kerr effect in the $(Co,Fe)_2B$ phase, although the easy-axis domain structure in this phase is most easily seen by the Bitter technique (Figure 2d). Apparently the easy magnetic axis, the tetragonal c-axis, coincides with the dendrite growth direction. For lower Fe contents, the $(Co,Fe)_2B$ has easy-plane magnetic symmetry, shows no polar Kerr effect, and collects little ferrofluid.

Nearly single-phase Co_3B can also be produced by crystallization of melt-spun amorphous ribbons of Co-24 at.% B (Figure 3). The large crystals (>100 μm) were present in the as-cast ribbon, as described elsewhere,[5] but the smaller crystals (1-20 μm) formed from the amorphous matrix on heating to 575 °C. Note that Co_3B is metastable at this temperature, which is well below the eutectoid decomposition temperature of 845 °C.

Evidence that Fe decreases the stability of the orthorhombic Co_3B phase is not unexpected, since there is no stable Fe_3B phase in the Fe-B equilibrium diagram. Although orthorhombic Fe_3B has sometimes been reported in crystallization of amorphous Fe-B alloys, the metastable bc tetragonal Fe_3B

Figure 3. Co-24 at.% B melt-spun ribbon after 20 min at 575 °C.

phase is usually the one observed. Bitter patterns on cast-in Fe_3B crystals[5] in Fe-24 at.% B ribbon (Figure 4a) indicate easy axis magnetic symmetry, with the tetragonal c-axis presumably the easy axis. Dark-field microscopy reveals magnetic domain patterns in the surrounding amorphous matrix (Figure 4b). Interpretation of these patterns[6] indicates that the matrix is in compression in the direction of the c-axis of the Fe_3B, and under tension in directions normal to this axis. These stresses presumably result from anisotropic differential thermal contraction between matrix and crystal on cooling, the Fe_3B c-axis contracting less, the a-axis more, than the matrix.

Crystallization of the amorphous matrix in Fe-24 at.% B at low temperatures produces fine crystals of tetragonal Fe_3B. However, heating this metastable phase to above about 600 °C leads to decomposition to the stable $Fe+Fe_2B$ phases.[1] We have found that substitution of as little as 2 at.% P for B can stabilize the tetragonal $Fe_3(B,P)$ phase in crystallized amorphous ribbons to at least 1000 °C, in agreement with the phase diagram of Rundqvist.[7] Chill-cast ingots annealed at 1000 °C for three days also consist predominantly of this phase, and the Bitter technique reveals that the grains in annealed Fe-23B-2P and Fe-20B-5P exhibit easy-axis magnetic symmetry. No Kerr domain contrast was seen in Fe_3B or $Fe_3(B,P)$.

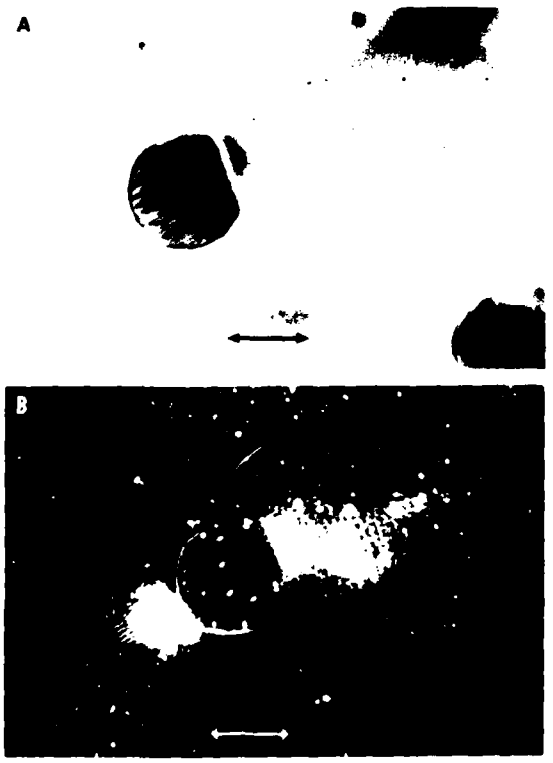

Figure 4. As-cast Fe-24 at.% B melt-spun ribbon with Bitter solution; (a) bright field, showing domains in cast-in Fe_3B crystals, (b) dark field, showing domains in adjacent amorphous matrix.

DISCUSSION

Magnetic domain patterns indicating substantial easy-axis magnetic anisotropy were seen in orthorhombic Co_3B and $(Co,Fe)_3B$ and in tetragonal Fe_3B and $Fe_3(B,P)$. They were not seen in Co_2B or $(Co_{.75}Fe_{.25})_2B$, but were seen in $(Co_{.5}Fe_{.5})_2B$. The latter observation is consistent with direct anisotropy measurements on $(Co,Fe)_2B$ compounds by Iga,[8] who found that the easy-plane symmetry of Co_2B changed to easy-axis with the substitution of sufficient Fe for Co.

The average width of surface domains on thick crystals can be used as a measure of domain-wall energy.[9,10] Using the method of Bodenberger and Hubert,[10] we estimate a wall energy of 17 ergs/cm^2 for Co_3B. This is intermediate between the wall energies of Co and Co_5Ce.[9]

Omori and Hashimoto[11] recently noted it is difficult to distinguish between Co_3B and Co_2B phases by optical microscopy. As shown in the present work, however, their different magnetic symmetries make it easy to distinguish between these phases by Kerr or Bitter techniques. Domains in easy-axis Co_3B have a significant component of magnetization normal to the surface, producing both a polar Kerr effect and significant ferrofluid collection. In easy-plane Co_2B, magnetization remains parallel to the surface, and neither effect occurs.

Metallographic observations indicate that substitution of Fe for Co decreases the temperature range of stability of the orthorhombic Co_3B phase. Substitution of P for B increases the stability of the tetragonal Fe_3B phase.

Identification of easy-axis magnetic anisotropy in boride phases with high Curie temperatures and magnetizations suggests them as possible candidates for permanent-magnet materials. However, direct measurements of anisotropy constants are necessary to assess fully their potential.

ACKNOWLEDGMENTS

We are grateful to J.L. Walter for providing various melt-spun ribbons, to W. Moore for alloy preparation, to G. Stebbins for directional solidification, and to S. Alessi and to J.L. Methe for excellent metallography. This work was supported in part by the Office of Naval Research.

REFERENCES

1. E. Coleman, *Mater. Sci. Eng. 39,* 261 (1971).
2. H.H. Liebermann, *IEEE Trans. Magn. MAG-15,* 1393 (1979).
3. R. Carey and E.D. Isaac, *Magnetic Domains and Techniques for Their Observation,* Academic Press, New York (1966).
4. S. Omori and Y. Hashimoto, *Trans. Jpn. Inst. Met. 17,* 571 (1976).
5. J.L. Walter, J.D. Livingston, and A.M. Davis, General Electric TIS Report 80CRD255.
6. J.D. Livingston, *Phys. Status Solidi A 56,* 637 (1979).
7. S. Rundqvist, *Acta Chem. Scand. 16,* 1 (1962).
8. A. Iga, *Japan. J. Appl. Phys. 9,* 415 (1970).
9. J.D. Livingston and M.D. McConnell, *J. Appl. Phys. 43,* 4756 (1972).
10. R. Bodenberger and A. Hubert, *Phys. Status Solidi A 44,* K7 (1977).
11. S. Omori and Y. Hashimoto, *Trans. Jpn. Inst. Met. 18,* 347 (1977).

DISTRIBUTION LIST

ORGANIZATION	COPIES
Defense Documentation Center Cameron Station Alexandria, VA 22314	12
Office of Naval Research Department of the Navy 800 N. Quincy Street Arlington, VA 22217 ATTN: Code 471	1
Code 470	1
Commanding Officer Office of Naval Research Branch Office Building 114, Section D 666 Summer Street Boston, MA 02210	1
Commanding Officer Office of Naval Research Branch Office 536 South Clark Street Chicago, IL 60605	1
Office of Naval Research Western Regional Office 1030 East Green St Pasadena, CA 91106	1
Naval Research Laboratory Washington, DC 20375 ATTN: Codes 6000	1
6100	1
6300	1
2627	1
Naval Air Development Center Code 606 Warminster, PA 18974 ATTN: Dr. J. DeLuccia	1

ORGANIZATION	COPIES
Naval Air Propulsion Test Center Trenton, NJ 08628 ATTN: Library	1
Naval Construction Battallion Civil Engineering Laboratory Port Hueneme, CA 93043 ATTN: Materials Division	1
Naval Electronics Laboratory San Diego, CA 92152 ATTN: Electron Materials Sciences Division	1
Naval Missile Center Materials Consultant Code 3312-1 Point Mugu, CA 92041	1
Commanding Officer Naval Surface Weapons Center White Oak Laboratory Silver Spring, MD 20910 ATTN: Library	1
Commander David W. Taylor Naval Ship Research and Development Center Bethesda, MD 20084	1
Naval Oceans Systems Center San Diego, CA 92132 ATTN: Library	1
Naval Underwater System Center Newport, RI 02840 ATTN: Library	1
Naval Postgraduate School Monterey, CA 93940 ATTN: Mechanical Engineering Department	1
Naval Weapons Center China Lake, CA 93555 ATTN: Library	1

ORGANIZATION	COPIES
Naval Air Systems Command Washington, DC 20360 ATTN: Codes 52031 52032	 1 1
Naval Sea System Command Washington, DC 20362 ATTN: Code 05R	 1
Naval Facilities Engineering Command Alexandria, VA 22331 ATTN: Code 03	 1
Scientific Advisor Commandant of the Marine Corps Washington, DC 20380 ATTN: Code AX	 1
Army Research Office P.O. Box 12211 Triangle Park, NC 27709 ATTN: Metallurgy & Ceramics Program	 1
Army Materials and Mechanics Research Center Watertown, MA 02172 ATTN: Research Programs Office	
Air Force Office of Scientific Research/NE Building 410 Bolling Air Force Base Washington, DC 20332 ATTN: Chemical Science Directorate Electronics & Materials Science Directorate	 1 1
Air Force Materials Laboratory Wright-Patterson AFB Dayton, OH 45433	 1
Library Building 50, Room 134 Lawrence Radiation Laboratory Berkely, CA	 1
NASA Headquarters Washington, DC 20546 ATTN: Code RRM	 1

ORGANIZATION	COPIES
NASA Lewis Research Center 21000 Brookpark Road Cleveland, OH 44135 ATTN: Library	 1
National Bureau of Standards Washington, DC 20234 ATTN: Metals Science and Standards Division Ceramics Glass and Solid State Science Division Fracture and Deformation Division	 1 1 1
Director Applied Physics Laboratory University of Washington 1013 Northeast Forthieth Street Seattle, WA 98105	 1
Defense Metals and Ceramics Information Center Battelle Memorial Institute 505 King Avenue Columbus, OH 43201	 1
Metals and Ceramics Division Oak Ridge National Laboratory P.O. Box X Oak Ridge, TN 37380	 1
Los Alamos Scientific Laboratory P.O. Box 1663 Los Alamos, NM 87544 ATTN: Report Librarian	 1
Argonne National Laboratory Metallurgy Division P.O. Box 229 Lemont, IL 60439	 1
Brookhaven National Laboratory Technical Information Division Upton, Long Island New York 11973 ATTN: Research Library	 1

Professor G.A. Ansell
Rensselaer Polytechnic Institute
Department of Metallurgical Engineering
Troy, NY 02181

Dr. C. Adam
Pratt & Whitney Aircraft Group
Government Products Division
P.O. Box 2691
West Palm Beach, FL 33402

Dr. E.M. Breinan
United Technology Corporation
United Technology Research Laboratories
East Hartford, CT 06108

Professor H.D. Brody
University of Pittsburgh
School of Engineering
Pittsburgh, PA 15213

Professor J.B. Cohen
Northwestern University
Department of Material Sciences
Evanston, IL 60201

Professor M. Cohen
Massachusetts Institute of Technology
Department of Metallurgy
Cambridge, MA 02139

Professor B.C. Giessen
Northeastern University
Department of Chemistry
Boston, MA 02115

Professor D. Turnbull
Harvard University
Division of Engineering and
Applied Physics
Cambridge, MA 02138

Dr. B.B. Rath
Naval Research Laboratory Code 6320
Material Science and Technology Division
Washington, DC 20375

Dr. N.C. Koon
Code 6632
Naval Research Lab
Washington, DC 20375

Professor N.S. Stoloff
Rensselaer Polytechnic Institute
School of Engineering
Troy, NY 12181

Professor A. Lawley
Drexal University
Department of Metallurgical Engineering
Philadelphia, PA 19104

Dr. F.E. Luborsky
Corporate Research and Development
General Electric Company
Schenectady, NY 12301

Professor C.D. Graham, Jr.
University of Pennsylvania
3451 Walnut Street
Philadelphia, PA 19104

Dr. J.J. Becker
Corporate Research and Development
General Electric Company
Schenectady, NY 12301

Professor D.G. Ast
Cornell University
Department of Materials Science and
Engineering
Ithaca, NY 14853

Professor O.D. Sherby
Stanford University
Materials Sciences Division
Stanford, CA 94300

Dr. K.S. Narasumhan
Crucible Research Center
P.O. Box 88
Pittsburgh, PA 15230

Dr. E.J. Yadlowsky
Kollmorgen Industrial Drives
801 First St.
Radford, VA 24141

D.L. Martin
759 Waite Road
Clifton Park, NY 12065

Dr. J.C. Williams
Carnegie-Mellon University
Department of Metallurgy and Materials Sciences
Schenley Park
Pittsburgh, PA 15213

Professor H.G.F. Wilsdorf
University of Virginia
School of Engineering and Applied Sciences
Charlottesville, VA 22903

R. Mehrabian
National Bureau of Standards
Metallurgy Division
Washington, DC 20234

Professor P.R. Strutt
University of Connecticut
School of Engineering
Department of Metallurgy
Storrs, CT 06268

Prof. R.W. Cahn
Laboratoire de Metallurgie Physique
Universite de Paris-Sud
91406 Orsay Cedex, FRANCE

Dr. H. Stadelmaier
North Carolina State Univ.
Dept. of Materials Engineering
Raleigh, North Carolina 27650

Dr. T.J. Dougherty
Columbia University
Chemical Engineering Research Labs
New York, NY 10027

Manfred Doser
Senior Development Engineer
Hitachi Magnetics Corp.
Edmore, MI 48829


ATE
LMED
8